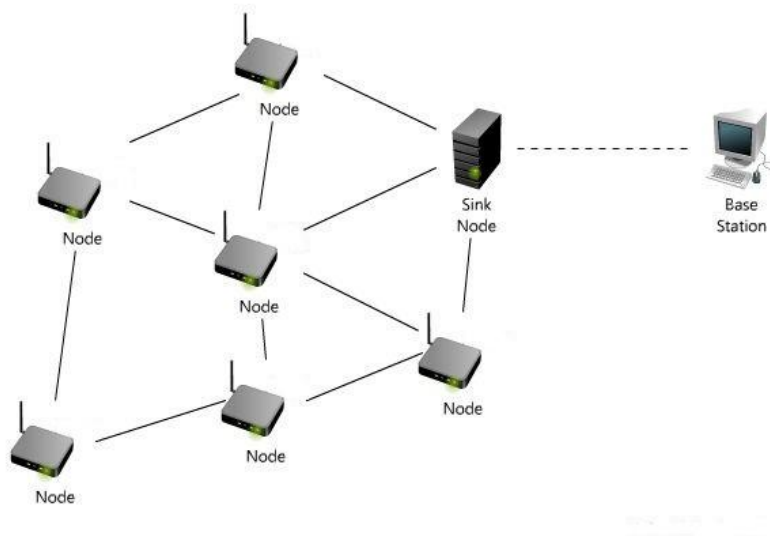


Routing Protocol for Wireless Sensor Networks with Hybrid Energy Storage System



Nuno André Saraiva Pais

Master Thesis

September 2009

Title:

Routing Protocol For Wireless
Sensor Networks with Hybrid
Energy Storage System

Project period:

January – September, 2009

Supervisors:

Dr. Neeli R. Prasad (np@es.aau.dk)
Dr. Fernando J. Velez (fjv@ubi.pt)

Co-Supervisors:

MSc. Bilge Cetin (bik@es.aau.dk)
MSc. Nuno Pratas (nup@es.aau.dk)

Number of reports printed: 3
Number of pages in report: 60
Number of pages in appendix: 2
Total number of pages: 62

ABSTRACT

This work presents new routing metrics for wireless sensor networks (WSNs) powered by harvesting sources. The models rely on a Hybrid Energy Storage System (HESS) which merges the complementarity of a Supercapacitor (SC) - low energy storage capability but perfect to handle high level of energy throuput and frequent charge cycles – and a Rechargeable Battery (RB) – higher energy storage capability but limited charge cycles. The HESS protocol assigns different metrics to the residual energy in both energy storage systems and favors routes with more SC energy and harvesting rates.

An energy model framework has been developped and simulated in MATLAB with different application scenarios. The results show that the balanced load of the energy consumption and the reliable delivery of data packets achieve an extension of the network lifetime using HESS flexible and energy aware cost function.

Table of Contents

LIST OF FIGURES.....	V
LIST OF TABLES	VI
LIST OF ABBREVIATIONS.....	VII
ACKNOWLEDGMENT	IX
1. INTRODUCTION.....	- 1 -
1.1 MOTIVATION	- 1 -
1.2 PROBLEM DEFINITION	- 1 -
1.3 GOAL OF THE PROJECT	- 2 -
1.4 ORGANIZATION OF THE THESIS	- 3 -
2. STATE OF THE ART	- 4 -
2.1 INTRODUCTION	- 4 -
2.2 ZIGBEE.....	- 4 -
2.3 STORAGE SYSTEMS	- 5 -
2.4 ENERGY HARVESTING	- 7 -
2.5 ROUTING PROTOCOLS	- 10 -
3. ENERGY AWARE ROUTING (EAR).....	- 14 -
3.1 INTRODUCTION	- 14 -
3.2 EAR DESCRIPTION.....	- 14 -
3.2.1 Setup Phase.....	- 15 -
3.2.2 Route Management.....	- 17 -
3.2.3 Data Dissemination.....	- 17 -
4. HESS MODELS.....	- 18 -
4.1 ENERGY MODELS	- 18 -
4.1.1 Analytical Model.....	- 18 -
4.2 POWER MANAGEMENT UNIT	- 20 -
4.3 COST FUNCTION.....	- 21 -
5. SIMULATION AND RESULTS.....	- 26 -
5.1 INTRODUCTION	- 26 -
5.2 NODE DEPLOYMENT.....	- 27 -
5.3 ROUTING TABLE	- 29 -
5.4 ENERGY STORAGE SYSTEM	- 29 -
5.4.1 Supercapacitor.....	- 29 -
5.4.2 Battery.....	- 30 -
5.5 RESULTS.....	- 30 -
5.5.1 Grid Deployment.....	- 31 -
5.5.2 Random Deployment	- 42 -
5.6 SUMMARY	- 44 -
6. CONCLUSIONS AND FUTURE WORKS.....	- 45 -
7. BIBLIOGRAPHY	- 47 -
8. APPENDIX	- 50 -
8.1 APPENDIX A: MATLAB CODE DESCRIPTION	- 50 -

8.1.1	<i>Node Deployment Setup.....</i>	- 50 -
8.1.2	<i>Routing Protocols Framework.....</i>	- 50 -

List of Figures

FIGURE 1.1 - NODE POWER SCHEME	2 -
FIGURE 2.1 - COMPARISON OF E-WME ALGORITHM TO ME AND MAXMIN ALGORITHMS (IN [13]).....	8 -
FIGURE 2.2 - NODE ENERGY DISTRIBUTION AFTER SENDING 4200 PACKETS (IN [13])	9 -
FIGURE 2.3 - NODE ENERGY DISTRIBUTION AFTER SENDING 1000 PACKETS (IN [13])	9 -
FIGURE 2.4 - (A) OLA FLOODING AND OLACRA, AND (B) LIMITED UPSTREAM FLOODING (OLACRA-FT) (NODES NOT SHOWN) (IN [19])	11 -
FIGURE 2.5 - SPIN PROTOCOL (IN [20])	12 -
FIGURE 3.1 - DIAGRAM OF A WSN.....	15 -
FIGURE 3.2 - EAR SETUP PHASE FLOWCHART	16 -
FIGURE 4.1 -POWER MANAGEMENT SYSTEM SCHEME.....	20 -
FIGURE 5.1 - RANDOM DEPLOYMENT WITH 150 NODES.....	27 -
FIGURE 5.2 - GRID DEPLOYMENT OF 64 NODES.....	28 -
FIGURE 5.3 - RESIDUAL ENERGY FOR THE SIMULATION A.....	31 -
FIGURE 5.4 - SUCCESSFUL PACKET FOR SIMULATION A	32 -
FIGURE 5.5 - PACKET DELAY IN <i>HOPCOUNTS</i> FOR SIMULATION A	32 -
FIGURE 5.6 - PACKET DELAY IN SECONDS FOR SIMULATION A	33 -
FIGURE 5.7 - NODE SELECTION ON A GRID DEPLOYMENT	33 -
FIGURE 5.8 - EAR SC RESIDUAL ENERGY DURING 12000 TIME SLOTS T (20 MIN)	34 -
FIGURE 5.9 - HESS SC RESIDUAL ENERGY DURING 12000 TIME SLOTS τ (20 MIN).....	34 -
FIGURE 5.10 - RESIDUAL ENERGY FOR SIMULATION B	35 -
FIGURE 5.11 - SUCCESSFUL PACKET DELIVERY FOR SIMULATION B.....	36 -
FIGURE 5.12 - PACKET DELAY IN <i>HOPCOUNTS</i> FOR SIMULATION B.....	36 -
FIGURE 5.13 - PACKET DELAY IN SECONDS FOR SIMULATION B	37 -
FIGURE 5.14 - PACKETS FORWARDED FOR SIMULATION C	38 -
FIGURE 5.15 - PACKET DELAY IN <i>HOPCOUNTS</i> FOR SIMULATION C.....	38 -
FIGURE 5.16 - PACKET DELAY IN SECONDS FOR SIMULATION C	39 -
FIGURE 5.17 - PACKET DELAY IN <i>HOPCOUNTS</i> FOR SIMULATION D	40 -
FIGURE 5.18- PACKET DELAY IN SECONDS FOR SIMULATION D.....	40 -
FIGURE 5.19 - DIFFERENTIAL RESIDUAL ENERGY WITH 64 NODES	41 -
FIGURE 5.20 - RANDOM DEPLOYMENT RESIDUAL ENERGY	42 -
FIGURE 5.21 - RANDOM DEPLOYMENT SUCCESSFUL PACKET.....	43 -
FIGURE 5.22 - RANDOM DEPLOYMENT PACKET DELAY IN <i>HOPCOUNTS</i>	43 -
FIGURE 5.23 - RANDOM DEPLOYMENT PACKET DELAY IN SECONDS	44 -

List of Tables

TABLE 2.1 - COMPARISON OF RECHARGEABLE BATTERIES (IN [8])	- 6 -
TABLE 2.2 - COMPARISON ON ENERGY HARVESTING DEVICES (PZ: PIEZO; ES: ELECTROSTATIC; EM: ELECTROMAGNETIC) (IN [12])	- 7 -
TABLE 4.1 - HESS COST FUNCTION PARAMETERS	- 21 -
TABLE 4.2 - WEIGHT DISTRIBUTION OF THE COST FUNCTION.....	- 23 -
TABLE 4.3 - PARAMETERS RESULTING IN THE MINIMUM COST FUNCTION	- 23 -
TABLE 4.4 - PARAMETERS RESULTING IN THE MAXIMUM COST FUNCTION.....	- 24 -
TABLE 5.1 - NUMBER OF DEPLOYED NODES IN A RANDOM SCENARIO	- 27 -
TABLE 5.2 - NUMBER OF DEPLOYED NODES IN A GRID SCENARIO	- 28 -
TABLE 5.3 - CHARACTERISTIC DATA FOR THE MICA2DOT SENSOR PLATFORM	- 30 -
TABLE 5.4 - GRID DEPLOYMENT SETUP FOR SIMULATION A	- 31 -
TABLE 5.5 - GRID DEPLOYMENT SETUP FOR SIMULATION B	- 35 -
TABLE 5.6 - GRID DEPLOYMENT SETUP FOR SIMULATION C	- 37 -
TABLE 5.7 - GRID DEPLOYMENT SETUP FOR SIMULATION D	- 39 -
TABLE 5.8 - RANDOM DEPLOYMENT SETUP	- 42 -

List of Abbreviations

ADV	Advertisement packet
AODV	Ad Hoc On Demand Distance Vector
BS	Base Station
CFP	Cost Function Packet
CFR	Cost Function Request
DoD	Depth of Discharge
E-WME	Energy-Opportunistic Weighted Minimum Energy
EAR	Energy-Aware Routing
HESS	Hybrid Energy Storage System
ME	Minimum Energy Routing
OLA	Opportunistic Large Array
RB	Rechargeable Battery
RREQ	Route Request
RREP	Route Reply
RPT	Report
RX	Reception
SC	Supercapacitor
SPIN	Sensor Protocols for Information via Negotiation
TX	Transmission
WSN	Wireless Sensor Network

Preface

This report has been written as a project for the 10th semester during the nine first months of 2009, in cooperation with the Center for TeleInFrastruktur (CTiF), headquartered in Aalborg University and Instituto de Telecomunicações (IT) from University of Beira Interior in Covilhã, Portugal.

The report is intended to the group with comprehension and understanding of the problem-based learning method, which is used at Aalborg University.

The report contains technical details. The literature references are marked by numbers in square brackets, e.g. [1]. The equations are marked by numbers in, e.g. Equation 3.1, where the first number indicates that the equation belongs to the second chapter, and the second number indicates that it is the first equation in this chapter. For the tables and figures, expression like Figures 4.1 is used, which has the similar meaning as the equation expression.

Acknowledgment

I would like to express my gratitude to my supervisors, Dr. Neeli Rashmi Prasad, Dr. Fernando José da Silva Velez, MSc. Bilge Kartal Cetin and MSc. Nuno Pratas, for their valuable guidance throughout this project and who together, enabled this amazing experience. I also acknowledge the fundamental collaboration of the members of the Center for TeleInFrastruktur (CTiF). I wish to express my love and gratitude to my beloved family; for their support and endless love, through the duration of my studies. A very special thanks goes to Ahmad R. Rostami; for his friendship and support, as well as to Ana Machado for her patience and affection.

In conclusion, I recognize that this work would not have been possible without the financial assistance of the MSc. grant assigned to me by Instituto de Telecomunicações and also the Student Mobility grant from the ERASMUS program.

Aalborg University, September 11th 2009

Nuno André Saraiva Pais

1. Introduction

1.1 Motivation

As miniaturization in Wireless Sensor Networks (WSNs) enables the entrance of this *Smart Dust* into our quotidian, energy issues are still one of the main concerns. The small sized nodes are supplied by ordinary non-rechargeable batteries which limit the lifetime of the network. The use of energy-aware routing protocols and low power nodes are not enough if the aim is to operate WSNs in isolated and unreachable places where battery exchange cannot be carried on.

Therefore, environmental energy is an attractive power source for low power WSNs. The photovoltaic technology is, by the most, the better energy source that can actually power self-sustainable sensor nodes in their habitat [1].

The development of an energy-aware routing protocol, which bases its routing decisions on the dynamic behaviour of the network, must be performed in order to extend the network lifetime.

1.2 Problem Definition

Energy is considered a factor of major importance in WSNs. The small size nodes are typically small and thus use tiny batteries which lead to short network lifetime. Harvesting devices can extend the network lifetime but nodes are still limited to the number of charge-discharge cycles of a Rechargeable Battery (RB) before its capacity falls below 80% of its initial rated capacity [2]. The network lifetime depends strongly on the residual energy of the nodes. It assumed that the network lifetime represents the period in which the all nodes are in operation until the first node drains all its energy causing its incapacity to communicate with its neighbours.

Meanwhile, based on the radio model proposed in [3], wireless communication requires much more energy consumption than sensing and computing tasks. Therefore it is desirable to use short-range instead of long-range communication between nodes because of the transmission power required. The energy awareness of the routing protocol is mainly the dictator of the network lifetime.

Another lifetime constraint is the unbalanced load of the data transmission which results in backbone formation. This state of the WSN occurs when several nodes want to route data to a Base Station (BS) or to a sink node through the same path. Some nodes can experience a total lack of energy when these are located in a backbone formation [4] while neighbours

can still have high levels of energy. So it is important to be aware of the routing queue along the data paths which also can cause delay and packet drops in the network. Energy-aware routing protocols play an important role in the next node selection avoiding crowded paths and low residual energy.

1.3 Goal of the Project

The aim behind this work is the lifetime extension of the WSN. In order to accomplish it, a harvesting device powers each node in association with a Hybrid Energy Storage System (HESS). The HESS is a crucial part of the node since it supplies all electronic components. The HESS is composed by a rechargeable battery (RB), a supercapacitor (SC), as well as a power management device that controls all the operations in the energy system. The power management has to tune-up the energy flow to optimize the lifetime of the node. This particular task will dictate the lifetime of the node. At the same time, it is necessary to buffer the RB with a SC in order to prevent constant and direct recharges of the RB which place significant stress on it,

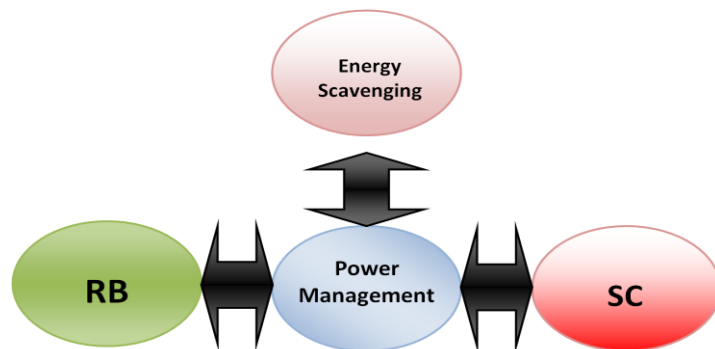


Figure 1.1 - Node Power Scheme

The other topic for the research is the routing protocol. It is well known that the routing protocol must fulfil the requirements of the application. But it is its responsibility to route the data packets all over the network and since main energy consumption is used in transmission, it is vital to optimize the data RX/TX. Routing data by the minimum hop count path may not be the best solution since it leads to a rapid exhaustion of that path. A proper solution must be formulated that consider energy cost function with appropriated parameters in order to transmit the data packets by the most high-energy nodes, in other words, transmit the data packets through nodes with higher harvesting rates and higher remaining energy levels.

1.4 Organization of the Thesis

The thesis is organized as follows. An overview of the related work is presented in Chapter 2 where energy storage systems are discussed and energy-aware routing protocols are analysed. Chapter 3 explains the Energy Aware Routing (EAR) protocol in its different steps. Chapter 4 presents the HESS framework developed. This formulation considers the energy models, the power management unit and the cost function. The simulation framework as well as the results are discussed and analysed in Chapter 5. The comparison between EAR and our version of HESS is possible because EAR was modified to include a hybrid energy storage system. Chapter 6 provides the conclusions and suggestions for further work.

2. State of the Art

2.1 Introduction

Wireless Sensor Networks (WSNs) consist of small nodes with sensing, computation, and wireless communications capabilities [5]. Many protocols have been developed, specially designed for WSNs since the number of applications is increasing at the same time that new developments are turning the nodes into “dust”.

However, most of the attention has been given to the energy awareness of the routing protocols since the major problem is still the node energy source and consequentially the lifetime of the network that depends of the application. In most scenarios, it is impractical to replace the batteries of the nodes since they can be deployed in a large area or even in unreachable places.

Different network structures according to the applications and the specifications of the sensing task have been created in order to extend the lifetime of the WSN. It can be defined three major groups of network structures; a flat structure where each node typically plays the same role and where they collaborate together to perform the sensing task; a hierarchical structure usually composed by a sink node, a router and the coordinator node where different tasks are addressed to different node; and location-based structure where the sensor nodes' positions are exploited to route data in the network.

The adaption of the network structure is always due to the applications requirements. Some applications demand a flat topology where nodes are free to move which results in unpredictable changes and where it needs equal privileges to a more adaptive network. Other applications require a hierarchical structure when special tasks are distributed through the nodes. This structure emphasizes the tree structure where each level represents a type of nodes that perform a specific task. In turn, the location coordinates may be important which supported by Global Positioning System (GPS) provide the exact position of nodes or group of nodes.

2.2 ZigBee

Most of the nodes available for Wireless Sensor Network (WSN) follows the ZigBee specification that is a suite of high level communication protocols using small, low-power digital radios based on the IEEE 802.15.4 standard [6]. ZigBee is targeted at radio-frequency applications that require a low data rate, long battery life and secure network.

The basic channel access mode is a carrier sense, multiple accesses with collision avoidance (CSMA/CA). This is explained as, the node checks briefly the channel to see that no one is talking before it starts transmitting. When the channel is occupied, it holds a back off time and then tries again. If the channel is still busy, it waits a higher back off time. This process can be carried on for 16 times, after that, if it was still impossible to send the packet, it will be dropped.

With this specification, the packet collision problem can be despised considering that the MAC layer of the ZigBee specification is collision avoidance.

2.3 Storage Systems

In order to operate a WSN, each node must have a power source to provide load to the electronic devices. Since it is frequently desirable to install nodes in inaccessible locations, it can be difficult to provide sufficient energy storage for long term operation or to replace the power source with regularity. Although the performance of non-rechargeable energy source, such as batteries and fuel cells, has improved over the years, their improvement is fairly gradual compared with other areas of electronics development and they cannot satisfy the demands for long life, low volume, low weight and limited environmental impacts [7].

Every electronic component needs to be powered by an energy source. In most of the cases, when devices need to be wireless, the energy source used is a battery. However, since the battery has a limited capacity, this one will discharge itself completely where it gets useless. In this situation, a battery switch needs to be carried on in order to maintain the serviceability of the system.

In some WSN applications (hazardous environments, environmental monitoring, etc), it is difficult or impossible to reach all nodes of the network. The solution might be the use of a self-sustainable source of energy in order to power the node. This can be obtained by harvesting energy from a power source (vibration, electromagnetic, etc).

In order to store the energy harvested, it is necessary to have a device able to store energy. The rechargeable battery is one of the devices that can actually perform this task.

Advances in battery technology have now resulted in quite a range of different rechargeable batteries from which to choose. This can make hard to decide which type is the best choice for some applications. Table 2.1 shows the main characteristics of the principal batteries available in the market.

Table 2.1 - Comparison of rechargeable batteries (in [8])

TYPE	NOMINAL CELL VOLTS	ENERGY DENSITY (Wh/kg)	CYCLE LIFE	CHARGING TIME	MAXIMUM DISCHARGE RATE	COST	PROS & CONS	TYPICAL APPLICATIONS
SLA	2.0	LOW (30)	LONG (Shallow cycles)	8 - 16h	MEDIUM (0.2C)	LOW	Low cost, low self-discharge; happy float charging; but prefer shallow cycling	Emergency lighting, UPSs, solar power systems, wheelchairs, etc
RAM	1.1	HIGH (75 initial)	SHORT TO MEDIUM	2 - 6h (pulsed)	MEDIUM (0.3C)	LOW	Low cost, low self-discharge; prefer shallow cycling; no memory effect but short cycle life	Portable emergency lightning, toys, portable radios and CD players, test instruments, etc
NiCad	1.2	MEDIUM (40-60)	LONG (Deep cycles)	14 - 16h (0.1C) OR < 2h with care (1C)	HIGH (>2C)	MEDIUM	Prefer deep cycling, good pulse capacity; but have memory effect; fairly high self-discharge rate	Portable tools & appliances, model cars & boats, data loggers, camcorders, portable transceivers & test equipment
NiMH	1.2	HIGH (60-100)	MEDIUM	2 - 4h	MEDIUM (0.2 - 0.5C)	HIGHER	Very compact energy source; but have some memory effect; high self-discharge rate	Cellphones & cordless phones, compact camcorders, laptops, PDAs, personal DVD & CD players.
Li-ion	3.6	VERY HIGH (> 100)	LONG	3 - 4h (1C + 0.03C)	MED/HIGH (<1C)	VERY HIGH	Very compact, low maintenance; low self-discharge; but need great care with charging	Compact cellphones & notebook PCs, digital cameras and similar very small portable devices

Since each type of batteries has singular characteristics, the choice remains on the applications and environment requirements.

Their huge capacity and low leakage, when compared to SCs, select them as great devices to the primary energy storage system. The bigger limitation is its fixed cycle life that is defined as the number of complete charge – discharge cycles a battery can perform before its nominal capacity falls under 80% of its initial capacity [2].

In order to maintain the idea of increased lifetime, the rechargeable battery must preserve its initial capacity as long as possible. Some studies show that repeated full discharges would lower the specified cycle life of the battery [9,2] so the challenge is to balance the shallow discharge of the battery with the aim of saving the energy system. One way to prevent the charge-discharge of the RB is to buffer volatile inputs from the energy source using a SC. In this way, the cycle lifetime of the RB is saved avoiding its premature deterioration.

The use of SCs as energy stores on WSN nodes is increasing [1,10], but their behaviour differs from that of batteries. Contrarily to the RB, a SC has a higher leakage; more cycle life (~ 1 million) but have a lowest capacity. These characteristics show that they are both complementary storage systems.

In normal use, a supercapacitor (SC) deteriorates to about 80 percent after 10 years [11], which gives it a long term lifetime.

2.4 Energy Harvesting

The most common issue in WSNs is the energy consumption that restricts the health-time of the network. One way to extend the lifetime of a WSN is doing energy harvesting using the free energy that surrounds us.

A good work has been done in [12] that gathered all the main energy harvesting systems sources to power a WSN and the result is shown in Table 2.2.

Table 2.2 - Comparison on energy harvesting devices (pz: Piezo; es: electrostatic; em: electromagnetic) (in [12])

Operating mode/material	Output power [μ W]	Frequency [Hz]	Amplitude [ms^{-2}]	Normalised Power [μ W]	Volume [mm^3]
Vibration - pz	2.1	80.1	2.3	0.5	125
Vibration – pz	210	120	2.5	28	1000
Vibration – pz	375	120	2.5	50	1000
Vibration – pz	0.6	900	9.81	0.0007	2
Vibration – es	3.7	30	50	0.005	750
Vibration – es	1052	50	8.8	27	1800
Vibration – es	70	50	9.2	1.7	32
Vibration - em	0.3	4400	382	4.7×10^{-8}	5.4
Vibration - em	180	322	2.7	7.7	840
Vibration - em	4000	100	0.4	25000	30000
PVDF shoe stave	-	-	-	1300	5000
PZT Dimorph	-	-	-	8400	1700
Em shoe insert	-	-	-	60000	56000
Em shoe insert	-	-	-	90000	97500
EAP shoe insert	-	-	-	1000000	50000
Thermoelectric	-	-	-	50	41
PV cell (outdoor)	-	-	-	20000	500000
PV cell (indoor)	-	-	-	1500	500000

It is shown in the previous table some kind of energy source and their respective available power. The most impressive energy source still is the photovoltaic energy that transforms the electromagnetic radiation in the region of the visible part of the spectrum into electrical energy. It has a good efficiency ratio of about 15%. In turn, the results presented for the Electro-Active Polymers (EAP) material is more suitable in the Wireless Body Area Network. It is a kind of material that when subjected to a strained, is capable to generate electrical power. The worst problem in this harvesting source is with the energy transference to the nodes since this scavenging device is applied on the foot. The electromagnetic vibration energy harvesters ranging from micro electro mechanical (MEM) devices also appears to be a suitable

choice since it is capable of converting up to 30% of the total energy supplied into useful electrical energy.

Some works have been published in the field of WSNs that use energy harvesting from the environment to increase their lifetime.

In [13], a routing protocol is presented that optimally utilizes the available energy – Energy-Opportunistic Weighted Minimum Energy (E-WME). The respective energy model, based in an energy storage system with a rechargeable battery, is the following:

$$P_n(\tau) = \min[P_n(\tau - 1) + \gamma_n(\tau - 1), u_n] - I(a_n(j)l(j)e_n(R(j))) \quad (2-1)$$

where,

- $P_n(\tau)$ - is the residual energy at the end of time slot τ ;
- $\gamma_n(\tau - 1)$ - is the energy harvested in the previous time slot;
- u_n - is the capacity of the battery on the n^{th} node;
- $a_n(j)$ - is a logical value indicating if the j^{th} node is on the route;
- $l(j)$ - is the length of the j^{th} packet in bits;
- $R(j)$ - is the route for the j^{th} packet;
- $e_n(R(j))$ - is the transmit and receive energy per bit consumed by the n^{th} node on the j^{th} packet. It depends on $R(j)$ because $R(j)$ indicates the distance to the next node, which in turn determines the transmit energy;
- $I(\cdot)$ - is the indicator function. It has value 1 if the route request including the j^{th} node is accepted and zero otherwise.

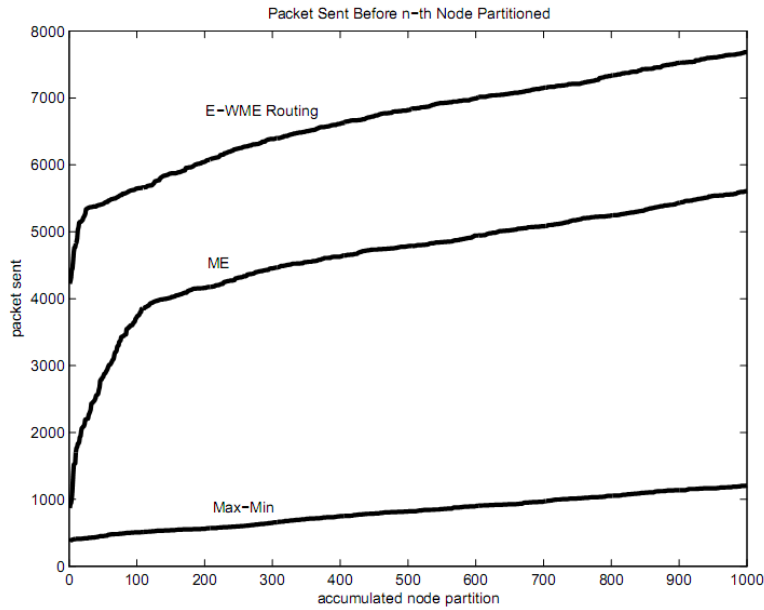


Figure 2.1 - Comparison of E-WME Algorithm to ME and Maxmin Algorithms (in [13])

When comparing the E-WME algorithm throughput with the minimum energy routing and the max-min routing one, it can be seen that the E-WME algorithm has always higher throughput.

The proposed algorithm also achieves better result than the Minimum energy algorithm when the node energy distribution after 4200 successful end-to-end packet deliveries is analysed. This corresponds approximately to the time-instance at which the first node partitions take place in E-WME.

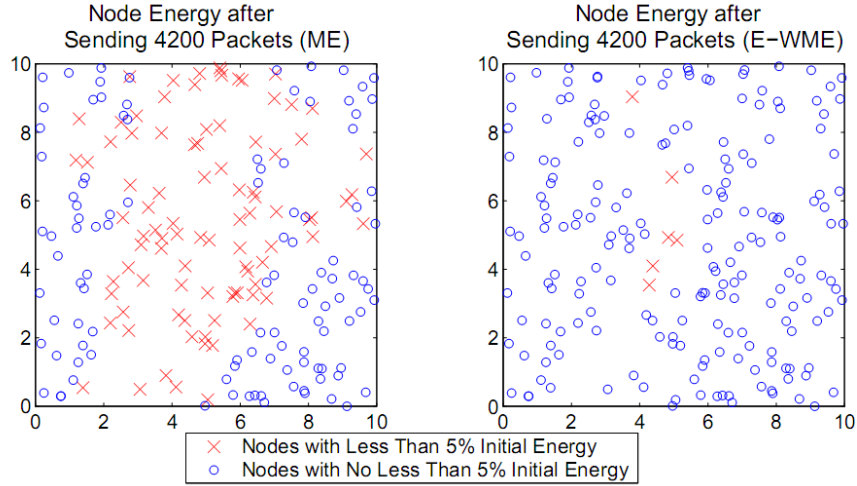


Figure 2.2 - Node Energy Distribution after Sending 4200 packets (in [13])

When compared with the Max-min algorithm, the E-WME routing protocol overcomes it much early, being necessary only 1000 packets to deplete the energy level of the Max-min nodes.

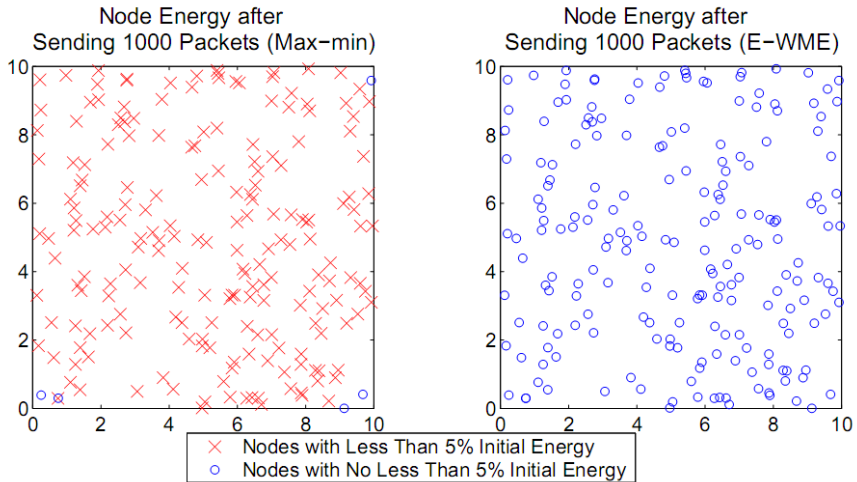


Figure 2.3 - Node Energy Distribution after Sending 1000 packets (in [13])

The reason for the poor performance of the Max-min algorithm is its failure to consider transmit and receive energies, which leads to routes with only few hops and very large average energy expenditure per packet [13].

One of the worst problems with the previous presented algorithm is that it recharges directly the battery when it experiences recharge cycles daily, placing significant stress on it. This limits the lifetime of the battery and therefore the lifetime of the entire network.

In [14], several approaches to improve battery runtime in mobile applications are shown. The use of SCs to extend the runtime of a mobile device is analysed for three different approaches. An overall reduction in the internal losses is possible by connecting SCs in parallel resulting in a run-time extension of 4% and 12%. Also in [14], it has been shown that the use of a dc-dc converter appears to be a cost effective option, since it allows the use of reduced number of capacitors while maintain a comparable performance.

The performance of a battery-supercapacitor hybrid power source under pulsed load conditions is also analytically described in [15] where the authors show that peak power can be greatly enhanced; internal losses can be considerably reduced; and discharge life of battery is extended. Greatest benefits are seen when the load pulse rate is higher than the system eigen-frequency and when the pulse duty is small. Adding a simple 23 F supercapacitor in parallel with a typical Li-ion battery of 7.2 V and 1.35 Ah capacity can boost the peak power capacity by 5 times and reduce the power loss by 74%, while minimally impacting system volume and weight, for pulsed loads of 5 A, 1 Hz repetition rate, and 10% duty.

Another routing metric is presented in [16] for a switched hybrid energy storage system (SHESS), comprising a SC and a RB. The word “switched” comes from the fact that the SC is never connected to the RB. This work also takes into account a cooperative transmission that work similarly as the OLA’s algorithm. Unfortunately, no results have been shown until now.

2.5 Routing Protocols

Routing protocols are fundamentals to a good performance of the network since they are responsible for the data dissemination through nodes. Different applications require different routing protocols applied to their specifications and the challenge is related with the energy consumption that directly affects the network lifetime.

The first routing protocols were basically flooding protocols where data packets are broadcasted to neighbours which worked as repeaters. In this type of protocols, data packets are disseminated through the network until either a maximum number of hops is achieved or the destination node receives it. Flooding is a reactive technique and does not require costly topology maintenance neither complex route discovery algorithms. However, it has several disadvantages concerning the energy consumption since a message is broadcasted through all the possible paths without control or organization. This leads to a rapid deflection of the network and bandwidth when sending

extra and unnecessary copies of data by sensors covering overlapping areas. The implosion, caused by duplicated messages sent to the same node, is the principal drawback of flooding. Another basic routing protocol is gossiping, it avoids the problem of implosion by just selecting a random node in its neighbour to send the packet rather than broadcasting it blindly. However, this causes large delays in propagation of data which, in the majority of the applications, is not acceptable. Other problem in this kind of protocol is that the message can never reach the destination node since the data packet is broadcasted at each node to the next random node [17].

An efficient flooding of the network is proposed in [18] with information, coming from a source which they refer to as the leader. The Opportunistic Large Array (OLA) routing, proposed in [18], is a type of technique where a group of nodes can combine their transmission power and achieve a longer transmission range. This leads to cooperative transmission that permits to transmit reliably to far destinations. The intuition is that each of the waveforms will be enhanced by the accumulation of the power due to the aggregate transmission of all nodes while, if kept properly under control, the random errors or the receiver noise that propagate together with the useful signals will cause limited deterioration in the performance. New versions of OLA's propagation technique takes advantage of the concentric ring structure of broadcast OLAs to limit flooding on the upstream connection.

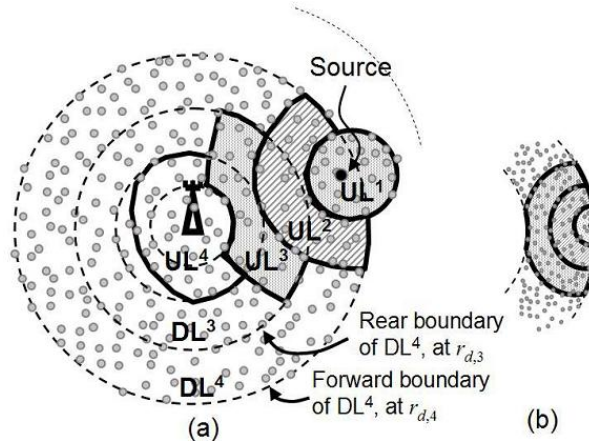


Figure 2.4 - (a) OLA flooding and OLACRA, and (b) limited upstream flooding (OLACRA-FT) (nodes not shown) (in [19])

The inconvenience behind these schemes lays on the fact that they require a high level of coordination achieved by synchronization. In turn, this cooperative transmission remains energy consumptions unconscious since the cost functions do not take into account any kind of residual energy or energy requirement to routing data. No harvesting process has been incorporated into this routing technique.

In many applications of sensor networks, it is not feasible to assign global identifiers to each node due to the large amount of random deployed

nodes. Therefore, it is hard to select a specific set of nodes to be queried. This consideration has led to data-centric routing, which differs from traditional address-based routing. Unlike traditional network communication, where individual nodes are named, data-centric communication relies on naming the data. This enables nodes within the network to store or cache the data transparently, as well as process the data. In this type of routing, the sinks send queries to certain sensed regions by sending metadata, called as attribute-based naming to specify the properties of the data. Sensor Protocols for Information via Negotiation (SPIN) is the first to consider data negotiation between nodes in order to avoid redundant data and save energy when compared with simple flooding.

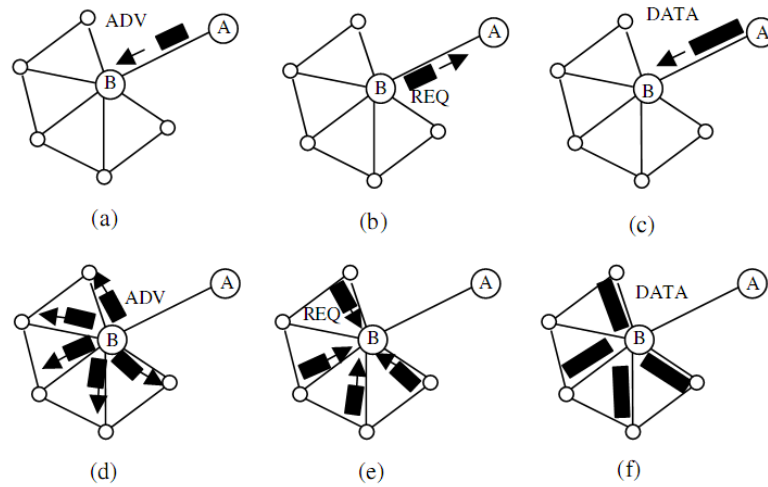


Figure 2.5 - SPIN Protocol (in [20])

One of the advantages of SPIN is the dynamic topology of the network since each node needs to know only its single-hop neighbours. With the negotiation protocol, SPIN reduces by 3.5 the energy consumed by the network when compared to flooding. Besides that, it uses almost halves the redundant data. However, SPIN cannot guarantee the delivery of data since there is no mechanism that refreshes the dissemination data in case of lost packet or unreached destination. Some protocols that follow the SPIN philosophy are presented in [21] and are tuned to different scheme networks. All of them use data-aggregation to avoid redundant data since they communicate with each other about the data that they already have and the data that they still have to obtain.

Directed Diffusion has also been developed and has become a breakthrough in data-centric routing. The idea is to diffuse data through sensor nodes by using a naming scheme for data getting rid of unnecessary operations of network layer routing in order to save energy [22]. Directed Diffusion queries the sensors in an on demand basis by using attribute-value pairs. It has also the possibility of choosing a path by selecting it by

reinforcement or eliminates it by negative reinforcement. Its aggregation and caching capabilities makes it highly efficient in terms of energy without the need for maintaining global network topology. However, Directed Diffusion cannot be applied to all applications as it is based on a query-driven data delivery model. Applications that need continuous data delivery won't work properly neither efficiently with a query-driven on demand data model. Furthermore, the unceasing reinforcement of a path will drop the energy source of the network rapidly, which will decrease the lifetime of the network.

Another on demand routing algorithm, named Ad Hoc On Demand Distance Vector (AODV), is presented by the authors of [23] but contrarily to the previous routing protocols, it is an IP-based protocol which in turn can also limit the number of nodes in the network. The disadvantage of this protocol is that it can easily consume all energy source for a frequently used path. In order to improve the lifetime of the network, some work has been done in [7] where they propose some energy models to distribute the power consumption among the nodes and then achieve better performance than the original AODV routing protocol. These energy models translate the energy consumption speed, the lifetime of each node and the remaining lifetime of the node. Based on their simulation results, the new metric has better performance than the original AODV routing protocols in terms of increasing the lifetime average of the whole network by around 5% in the hierarchical WSN, and around 10% in the flat network. Although these results may not be very expressive, a new research topic appears; the use of AODV protocol with cost functions that take into account the energy consumption per node and a hybrid storage system that is made of a RB and a SC, both of them recharged by an energy harvesting source.

3. Energy Aware Routing (EAR)

3.1 Introduction

The WSN have practical benefits that will improve the quality of life and also productivity and efficiency in the work environment.

Looking from a higher layer perspective, the sensors are generally equipped with data processing and communication capabilities. The sensing circuitry measures ambient conditions related to the environment surrounding the sensor and transform them into an electric signal. This information needs then to be sent to a sink node by a direct link (single hop) or broadcasted through the network using several intermediate nodes (multi hop). The sensor nodes are constrained in energy supply and bandwidth. Since most of the energy consumption is due to communication requirements, the load balance on the network must be as distributed as possible to extend the lifetime of the network.

Such constraints combined with a typical deployment of large number of sensor nodes have raised many challenges to the design and management of sensor networks. These challenges require energy-awareness at all layers of the networking protocol stack.

3.2 EAR Description

In order to route the packets through the network, it is essential to use a routing protocol that is energy-aware, and is ZigBee compliant. The Energy Aware Routing (EAR) protocol presented on [24] proposes a network where nodes generate messages containing information that is of interest of the network users and through multi-hop routing, forward these messages to the hubs in the network. A hub or sink node is a special node equipped with an additional communication technology to route the sensing packets to the Base Station (BS). The sensing nodes will send all messages to the hub or sink node for processing before further disseminating them to the network users located at the base station.

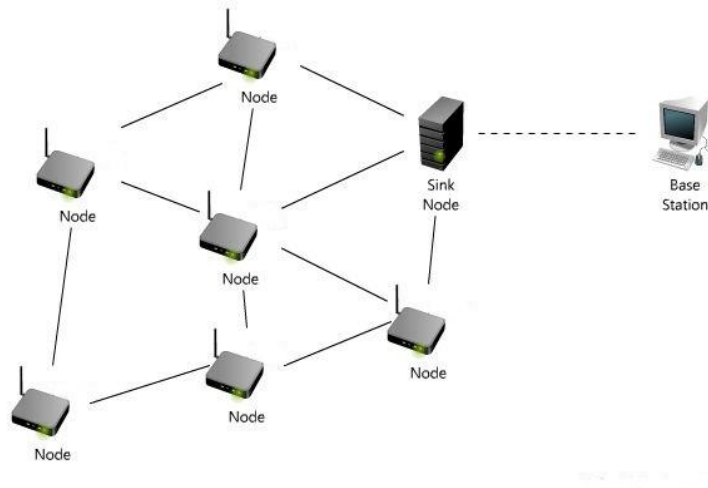


Figure 3.1 - Diagram of a WSN

In all sensor network applications, reliable and fast delivery of messages can be a major requirement. Based on this, the EAR protocol present an efficient and reliable routing protocol that routes packets to the sink node reliably and quickly using lightweight mechanisms that require little maintenance and control messages to handle a rapidly changing of topology and route maintenance.

3.2.1 Setup Phase

The setup phase of the EAR protocol handles with the routing table replenishment of each node. It will be filled with at least a route to the sink node in order to route the sensing packets. This is carried on with the broadcast of control packets that carries route information concerning the sink node.

The setup phase starts with a hub broadcast of an Advertisement (ADV) packet indicating that it wants to receive Report (RPT) packets generated by nodes. When neighbouring nodes around the hub receive this ADV packet, they will store this route in their routing table.

The nodes will then wait a random time before starting the initialization process. Therefore, a portion of nodes will receive route information before they have begun their initialization process. This enables fast propagation of route information and reduces the amount of control packets generated in the setup phase, reducing the setup phase time as well as the energy consumption by the control packets. So, randomly, the nodes start their initialization process by broadcasting a Route Request (RREQ) packet asking for a route to any hub. If a hub receives a RREQ packet, it will broadcast a Route Reply (RREP) packet. Similarly, when a node receives a RREQ packet, it will broadcast a RREP packet if it has a route to a hub. Otherwise, it will ignore the RREQ packet. The nodes do not need to propagate RREQ packet. This would delay the setup phase and the energy

consumption. The route information is taken into account by the random waiting time.

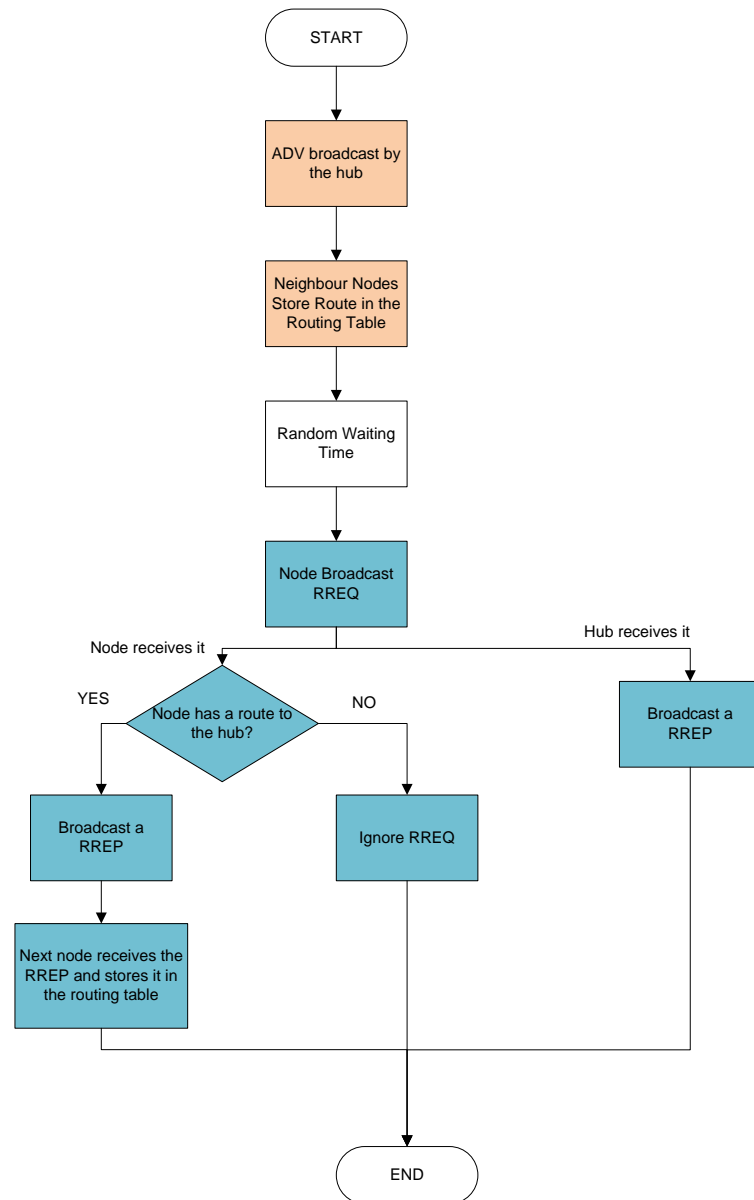


Figure 3.2 - EAR Setup Phase Flowchart

Each node will store more than one route to the hub. The route in the routing table is indexed by the next node's ID that is the neighbour of this node and by the path length or hop count that the packet will have to be relayed until it reaches the hub. This information is available in each routing table since the control packets broadcast is started by the hub and extended to the external zones of the network, always carrying the path length.

3.2.2 Route Management

The main EAR metric used by the authors of [24] is the *RouteScore*:

$$RouteScore = P_E \cdot W_E + P_L \cdot W_L, \quad (3-1)$$

where:

- P_E - energy level of the next hope node;
- W_E - assigned weight for P_E ;
- P_L - link quality to the next hope node;
- W_L - assigned weight for P_L .

The *RouteScore* takes values from 0 and 100 and higher values indicate a better route.

The packets are usually routed through nodes with higher *RouteScore*. All the routes stored in the routing table must be refreshed in order to choose the higher *RouteScore*. In order to accomplish this, a feedback packet is transmitted from the neighbours with a packet length of one byte each time and for every neighbour.

3.2.3 Data Dissemination

After the EAR initialization phase, each node will have at least one route to the hub. At this time, the nodes will start sensing the environment and generating RTP packets. When a RTP packet is generated at the source, it is set with two fields by EAR in its header; *ExpPathLen* and *NumHopTraversed*. As explained by the authors of [24], the first field defines the expected number of hops that the packet needs to traverse before it reaches the hub. This is possible since each node routing table stores the next node's ID and the respective path length or hop count until the hub. The packet is then queued into the output buffer of the node before being forwarded to the next node in the route. As soon as the packet is forwarded to the next node, the second field of the header (*NumHopTraversed*) is increased by one which has been initialized to 0. This gives historical information about the packet which can be used to control the delay. With this mechanism, the packet is constantly analysed in order to check if the *ExpPathLen* has been overcome, i.e., if the *NumHopTraversed* is larger than the *ExpPathLen*. If this occurs, the packet will be routed through the shortest path by selecting the nodes with lower *hopcount* to the hub. Otherwise, the packet is routed through the route with higher *RouteScore*.

4. HESS Models

4.1 Energy Models

Energy models for the HESS are based on the work of the authors from [25]. They already consider cycle life of the battery and hybrid energy harvesting system. Their work is based on the work of the authors in [13] which propose a cost metric that takes into account the nodes' Rechargeable Battery (RB) residual energy, harvesting rate and energy requirement for routing the packet.

4.1.1 Analytical Model

The wireless network is described by a directed graph $G(V, E)$, where V is the set of vertices that represent the sensor nodes of the network, and E is the set of edges that represent the communication links between nodes.

A 2-tuple (t_{nm}, r_{nm}) is related with each edge $(n, m) \in E$, where t_{nm} is defined as the transmission energy requirement per byte for node n and r_{nm} is the reception energy requirement per byte for node m . So, if a data packet of length l (in bytes) is sent from node n to m , an energy requirement of lt_{nm} to transmit the packet is subtracted from the energy storage system of node n and lr_{nm} is subtracted from the energy storage system of the receptor, node m . The same process occurs when Cost Function Packet (CFP) are exchanged between nodes which is explained in Chapter 4.3.

Therefore, it is defined the unit energy requirement of node n on path R as:

$$e_n(R) = r_{n''n} + t_{nn'}, \forall n \in R \quad (4-1)$$

Where nodes n'' and n' are the upstream and downstream neighbours of node n in path R , respectively. For adaption, the energy model for each node turns into $r_{n''n} = 0$ for source node and $t_{nn'} = 0$ for the destination node.

The authors in [13] considered that the transmission and the reception energy cost are nearly the same which is supported by the authors of [26]. However, as mentioned in Chapter 2.5, the routing layer has a very important role on the control of the energy expenditures, so it must not be neglected. An analysis of the energy consumption in Mica2dot sensor platform showed that the energy requirement per byte in a data transmission is nearly two times more than in a data reception [27]. Therefore, it becomes clear that the energy spent in TX and RX will depend on the wireless platform, and so, it must be differentiated.

This project considers a discrete-time system where each node supplies and harvests energy. At the beginning of each time slot τ , node n receives the harvested energy, accumulated in the previous time slot represented by $\gamma_n(\tau - 1)$. At the end of each time slot, the energy required to route the data packet is instantaneously removed from the energy storage system.

This thesis proposes the HESS which relies on a dual energy storage system represented in Figure 4.1. The work presented by the authors of [13] considers an energy storage system composed by a RB which must be developed in order to extend its model to a hybrid energy storage system.

The HESS energy model is structured into two parts: the availability to supply the transmission and the residual energy of each energy storage system at the beginning and at the end of time slot τ .

Therefore, the energy model for the SC at node n can be summarized by the following equations:

$$\hat{E}_{load,SC}(n, \tau, R(j)) = l(j)E(n, R(j)) \cdot I(\hat{E}_{SC}(n, \tau) - l(j)E(n, R(j)) > 0) \quad (4-2)$$

$$\hat{E}_{SC}(n, \tau) = \min[(E_{SC}(n, \tau) - \alpha(\tau - 1)) + [1 - S_2(n, \tau)]\gamma_n(\tau - 1), u_{SC}] \quad (4-3)$$

$$E_{SC}(n, \tau) = \beta(n, D, \tau)[\hat{E}_{SC}(n, \tau) - \hat{E}_{load,SC}(n, \tau, R(j))] \quad (4-4)$$

where $\alpha(\tau - 1)$ denotes time-invariant fraction of energy leaked in the SC over a time slot. u_{SC} describes the maximum capacity of the SC, and $\min[\dots]$ prevents the possibility of exceeding it. The residual energy in the SC at the beginning of time slot τ is presented by $\hat{E}_{SC}(n, \tau)$. The energy consumed by a packet if SC is used is given by $\hat{E}_{load,SC}(n, \tau, R(j))$ and is specific for each node at each time slot. The $l(j)$ represents the length of the j^{th} packet in bytes. Since $E_{SC}(n, \tau)$ denotes the residual energy in the SC at the end of time slot τ , $\beta(n, D, \tau)$ works only like an indicator function for the event that the RB on node n has not exceeded its finite cycle life. It is important to notice that $\beta(n, D, \tau)$ is a non-increasing function of τ , and for a fixed τ , is a strictly decreasing function of D , which represents the Depth of Discharge (DoD) on the RB. For example, if it is assumed to never use more than 30% of the RB energy within a single discharge cycle, then $D = 0.3$. The authors of [2] express DoD as a percentage, e.g., $D \times 100\% = 30\%$, it will be adopt in this work. The expression $I(\hat{E}_{SC}(n, \tau) - l(j)E(n, R(j)) > 0)$ indicates that the requested energy is enough to satisfy the request.

The energy model for the RB follows the previous logic and is expressed by the following expressions:

$$\hat{E}_{load, RB}(n, \tau, R(j)) = l(j)E(n, R(j)) \cdot \{1 - I[\hat{E}_{SC}(n, \tau) - l(j)E(n, R(j)) > 0]\} \cdot I[\hat{E}_{RB}(n, \tau) - l(j)E(n, R(j)) > (1 - D)u_{RB}] \quad (4-5)$$

$$\hat{E}_{RB}(n, \tau) = \min[E_{RB}(n, \tau) + S_2(n, \tau)\gamma_n(n, \tau - 1), u_{RB}] \quad (4-6)$$

$$E_{RB}(n, \tau) = \beta(n, D, \tau)[\hat{E}_{RB}(n, \tau) - \hat{E}_{load, RB}(n, \tau, R(j))] \quad (4-7)$$

where $\hat{E}_{RB}(n, \tau)$ represents the residual energy at the beginning of time slot τ . u_{RB} is the maximum capacity of the RB and it is minimized by the function $\min[\dots]$, preventing the RB of exceeding its maximum capacity. $\hat{E}_{load, RB}(n, \tau, R(j))$ is the energy consumed on node n by the j^{th} packet if the SC is used. $I[\cdot]$ is the indicator function. It assumes one if the route request is powered by the RB and zero otherwise. The RB will only supply the communication if its residual energy is above the DoD.

4.2 Power Management Unit

The new nodes powered by a hybrid energy storage system require a specific power management unit. This component controls the energy flow of the node and tunes it. A simplified scheme of HESS is shown in Figure 4.1.

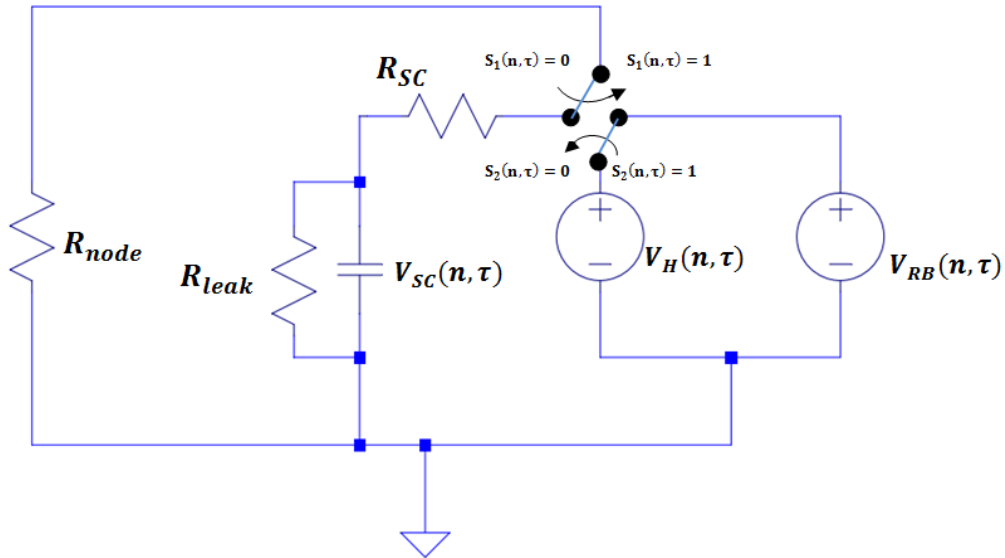


Figure 4.1 –Power Management System Scheme

It is assumed that the harvested energy $V_H(t)$ is directed to the SC ($S_2(n, \tau) = 0$) until the RB does not reach its designed DoD. Otherwise, the RB will be recharged until it gets full replenishment ($S_2(n, \tau) = 1$). This allows a better control of the cycle life of the battery.

As soon as a node is selected to relay a packet, it checks its residual energy and selects the appropriate energy storage to route data. By default, the SC is the main supplier of the node ($S_1(n, \tau) = 0$). This is due to the internal energy loss caused by a fast rate of current leakage which limits the time energy storage of the capacitor. Batteries also have an internal current leakage, but it is at a considerably slower rate. The authors of [28] studied the self-discharge rate of the supercapacitor applied in the context of WSN. They showed that the SC leakage is much higher than RB leakage and depends highly on the residual energy.

4.3 Cost Function

The goal of this work is to extend the lifetime of the network as much as possible. Therefore, it is important to balance the energy consumption of the network without affecting the delay. Since the routing protocol bases its decisions in cost functions, a reliable and light metric must be formulated.

The authors from [13] developed a metric which treats RBs with infinite cycle life and 100% DoD. Their metric is asymptotically optimal in terms of the competitive ratio and increases exponentially with the energy depletion, discouraging the use of a node with a low harvesting rate. The metric of [25] already takes into account the lower DoD of the RB as well as its cycle life time. However, both of them have a complex computation requirement which reflects in the energy consumption.

This work proposes a light cost function that evaluates the cost of routing a packet through a specific node. The metric is used whenever a node wants to route a data packet to its neighbours. The cost is sent back to the original node which analysis and selects the node with the lower cost function.

Since the cost function defines the network behaviour, it is highly recommended to select wisely the next node. To insure an extended lifetime of the network, the cost function must reflect the node ability to forward the packet through high SC residual energy nodes and high harvesting energy rates. Table 4.1 presents the parameters in HESS cost function.

Table 4.1 - HESS Cost Function Parameters

Symbol	Description
hc	<i>Hopcount</i>
e_{sc}	SC residual energy
e_{rb}	RB residual energy
γ	Harvested energy in the last time slot
L_c	Cycle life of the battery
$queue_{oc}$	Occupation of the transmission queue

This set of information, gathered in the cost function, translates the individual capability to route data packets:

- **hopcount (hc)** represents the (minimum) path length between the queried node and the hub/sink node. This information is set up in the routing table, at the EAR setup phase. This parameter gives the information about how far the next node is from the hub/sink node;
- e_{sc} and e_{rb} represent the residual energy of the SC and RB, respectively;
- γ gives the harvested energy that the node scavenged in the last time slot $(\tau - 1)$;
- L_C translates the RB cycle life time;
- **queue_{oc}** is the length occupation of the node's transmission queue.

The cost function which reflects the cost to route data can therefore, be summarized by the following equation:

$$Cost(n) = (hc(n) * w_{hc} + queue_{oc}(n) * w_{queue_{oc}}) - (e_{sc}(n) * w_{sc} + * w_{L_c} + e_{rb}(n) * w_{rb} + \gamma(n) * w_{\gamma} + L_C(n) * w_{L_C}) \quad (4-8)$$

The polynomial equation, representing the cost, carries two kinds of information: desirable or positive parameters which stands for parameters that support the extension of the network (residual energies, harvested energy and RB cycle life); and undesirable or negative parameters which should be as low as possible (hopcount and transmission queue). This reflects the formulation of the cost function in two separated terms. The first term returns the negative influence and the second minimizes it. Each parameter takes on a value from 0 to 100. For example, if $e_{rb} = 100$, it means that the RB residual energy is fully charged.

Each parameter has an associated weight. This allows a priority scheme in the cost function calculation. The weights are set as follows:

$$w_{hc} + w_{queue_{oc}} = 1.0 \quad (4-9)$$

$$w_{sc} + w_{rb} + w_{\gamma} + w_{L_c} = 1.0 \quad (4-10)$$

A weight distribution has been made based on the priority of each parameter in

Table 4.2.

Table 4.2 - Weight Distribution of the Cost Function

Positive Parameters	Negative Parameters
$w_{sc} = 0.45$	$w_{hc} = 0.5$
$w_{rb} = 0.2$	$w_{queue_{oc}} = 0.5$
$w_{\gamma} = 0.15$	-
$w_{L_c} = 0.2$	-

The SC residual energy weight gets the maximum weight since this energy is volatile and suffers from leakage problems. The RB characteristics (RB residual energy and cycle life) are assigned with a 20% of importance ending with a 15% of importance for the harvesting energy weight. Both of the “negative” parameters share a 50% of responsibility in the cost function result.

This scheme of weight can easily be adapted to different application scenarios. For example, WSN applications that have lower harvesting energy rates can assign higher weight to w_{γ} in order to customize the data flow. This formulation turns the HESS cost function into a flexible metric.

Whenever a node wants to route a data packet, it sends a Cost Function Request (CFR) to its neighbours. The neighbours will retrieve a Cost Function Packet (CFP) with the cost associated with the packet transmission.

Since the CFP will be transmitted by the neighbour nodes in each routing process, this will lead to a consumption of energy during the transmission. In order to reduce as much as possible the energy consumption and keep a good level of accuracy, it has been settled that the CFP, which is the response to the query of cost function, will be made of eight bits.

4.3.1.1 CFP Normalization

In order to reduce the communication energy consumption, a normalization of the cost function as been made. One byte packet seemed to be the appropriate length of a packet to retrieve the cost function to the sender node while still keeping a high level of accuracy and differentiation.

So the minimum cost function can be calculated by using the values from Table 4.3.

Table 4.3 - Parameters Resulting in the Minimum Cost Function

Positive Parameters	Negative Parameters
$sc = 100$	$hc = 2$
$rb = 100$	$queue_{oc} = 0$
$\gamma = 100$	-
$l_c = 100$	-

This situation produces the following cost:

$$Cost_{min}(n) = (2 * 0.5 + 0 * 0.5) - (100 * 0.45 + 100 * 0.2 + 100 * 0.15 + 100 * 0.2) = -99.0 \quad (4-11)$$

Equation (4-11) represents the situation of a node that is at two hops of the hub and has no queue occupation and full residual energy storage. The *hopcount* will never be lower than two because the transmission to the hub is ensured since the hub or sink node is the last node in the chain and warranties unlimited energy.

The maximum cost function can also be calculated and represents a node that has reached the end of its lifetime. Table 4.4 presents the respective weights.

Table 4.4 - Parameters Resulting in the Maximum Cost Function

Positive Parameters	Negative Parameters
$sc = 0$	$hc = 100$
$rb = 50$	$queue_{oc} = 100$
$\gamma = 0$	-
$l_c = 0$	-

The cost function can be calculated as follows:

$$Cost_{max}(n) = (100 * 0.5 + 100 * 0.5) - (0 * 0.45 + 50 * 0.2 + 0 * 0.15 + 0 * 0.2) = 90.0 \quad (4-12)$$

The battery still has half of its maximum capacity but since the DoD is set to 50%, the node dies.

So, for a data packet of eight bits, 256 different combinations translate the cost of routing the data packet through node n .

The limits of the cost are:

$$Cost(n) \in [-99; 90] \quad (4-13)$$

And the final result must use 8 bits, so there are $2^8 = 256$ different combinations.

$$Cost'(n) \in [0; 256] \quad (4-14)$$

In order to adjust the limits of the result, it is necessary to make a normalization of the initial result:

$$\frac{256-0}{90-99} = \frac{256}{189} \cong 1.3545 \quad (4-15)$$

So, the new cost function will be:

$$Cost'(n) = (Cost(n) - (-99)) * 1.3545, \forall Cost \in [-99; 90] \quad (4-16)$$

5. Simulation and Results

5.1 Introduction

In order to simulate the HESS performance, the routing protocol was implemented in MATLAB. The choice of the MATLAB simulator is made based in the author's previous experience. Other simulators, like Omnet++ or ns-2, were also suitable for the simulation development but their learning curves were out of the work time plan.

Therefore, the HESS metrics were created and developed under MATLAB programming language. It was expected that the HESS cost function would allow WSNs to extend their lifetime without compromising the delivery of data to the hub/sink node. Hence, in order to prove it, the following metrics were analysed:

- The residual energy of the network, as presented in Chapter 3, is represented and shown as distributed as possible along the network. This also concerns the ability of nodes with higher energy levels or harvesting rates in the network to provide routing capability to their neighbours, resulting in a flat or homogeneous consumption of energy;
- The successful and reliable delivery of packets to the hub/sink node. The packet latency is analysed resulting in the average time it takes a packet to be routed to the sink node. This analysis gathers the number of hops a packet had to traverse before it reaches the sink node (*hopcount*) as well as its average time;
- The data packets that are in the routing queue of each node waiting for being routed.

The results obtained with the HESS routing metric are analysed by considering the EAR metric, *RouteScore*, which is explained in Chapter 3. Since the energy storage system, presented by the authors of EAR, does not take into account a dual energy storage system (which is the case of HESS), a modification of the EAR protocol has been proposed. This change relies on a fair comparison between the two routing protocols that is achieved by adding a hybrid energy storage system to the EAR simulation. A full use of the SC residual energy is applied in EAR simulations and the RB recharging only occurs when the RB is fully discharged.

5.2 Node Deployment

Several types of node deployment have been chosen to analyse both routing protocols performance.

In large deployment scenarios, the huge amount of manpower to deploy each node is unpractical. A distribution by airplane is more suitable and a random distribution of nodes along an area arises. It has been defined a 200×200 m field of nodes where a hub/sink node is placed at the centre of the field (100,100). Figure 5.1 represents this scenario.

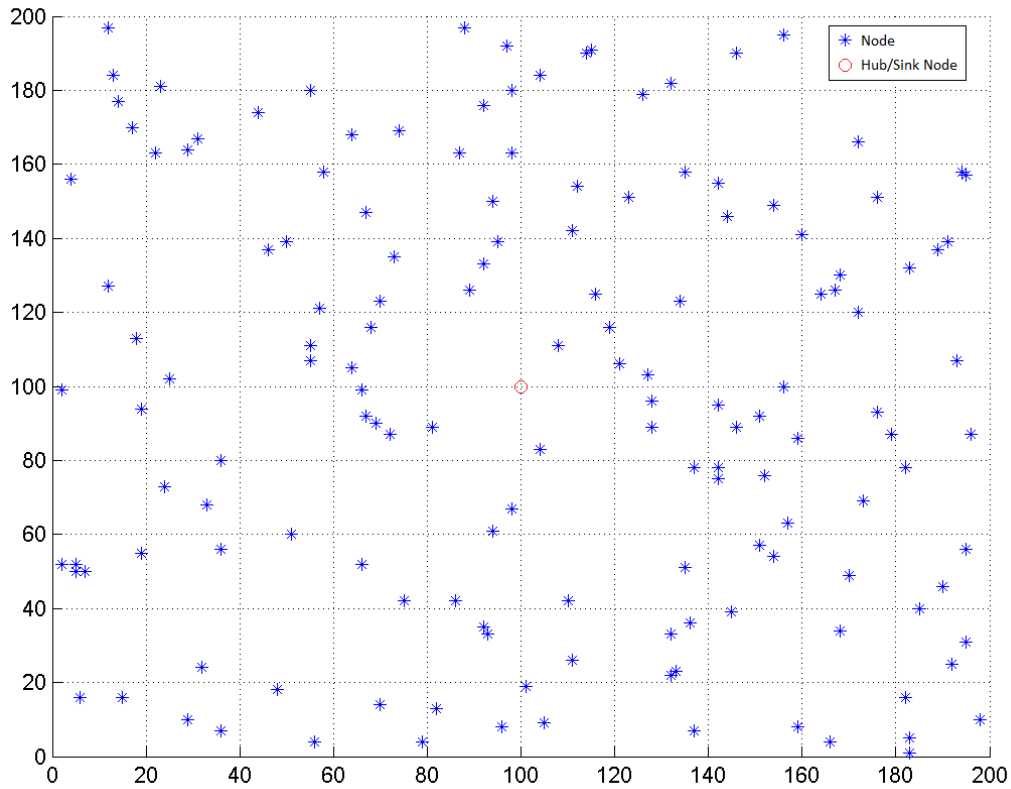


Figure 5.1 - Random Deployment with 150 Nodes

This scenario has been simulated with four network sizes, in terms of the number of nodes, in a fixed area (200×200 m). Table 5.1 represents the number of nodes deployed as well as the node density.

Table 5.1 - Number of Deployed Nodes in a Random Scenario

Number of Nodes	Node Density
50	$0.00125 \text{ nodes.m}^{-2}$
100	$0.0025 \text{ nodes.m}^{-2}$
150	$0.00375 \text{ nodes.m}^{-2}$
200	$0.005 \text{ nodes.m}^{-2}$

Since each deployment results in a different distribution scenario, several simulations needed to be carried out and the results were averaged. However, a complex and unrelated data resulted from the study of this scenario.

So, a simpler approach was chosen in order to interconnect the different nodes deployment results. A grid deployment seemed to be the perfect scenario to simulate and compare both routing protocol. Figure 5.2 represents the grid deployment.

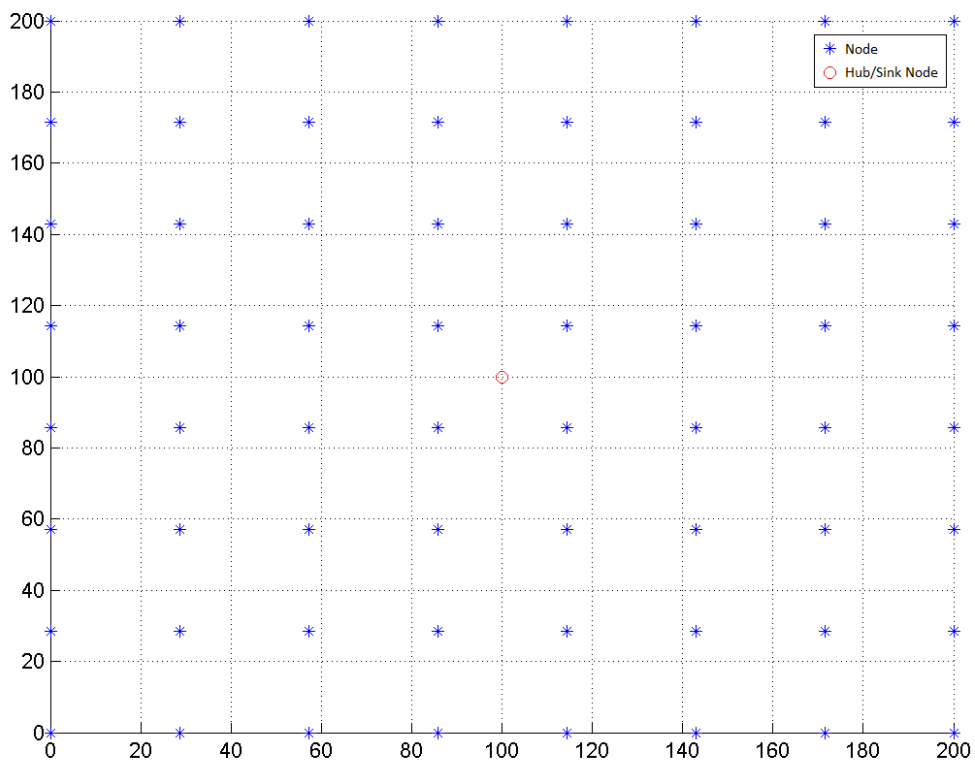


Figure 5.2 - Grid Deployment of 64 Nodes

A hub/sink node was placed at the centre of the deployment field with $200 \times 200\text{m}$ of area. Table 5.2 presents the three different network sizes as well as their node density used for the grid scenario simulation.

Table 5.2 - Number of Deployed Nodes in a Grid Scenario

Number of Nodes	Node Density
36	$0.0009 \text{ nodes.m}^{-2}$
64	$0.0016 \text{ nodes.m}^{-2}$
100	$0.0025 \text{ nodes.m}^{-2}$

5.3 Routing Table

As explained in Section 3.2.1, nodes store routing tables with the next hop node's Ids and the respective path length until the sink node.

Since the simulations are performed on a 200×200 m field, the maximum node density will occur with 200 nodes, as presented in Table 5.1, and will be:

$$A_{field} = 200 * 200 = 40000 \text{ m}^2 \quad (5-1)$$

$$Node_{density} = 200/40000 = 0.005 \text{ nodes.m}^{-2} \quad (5-2)$$

The radio range considered is 56 m and represents the radio coverage of each node. The range is based on [24] and give the opportunity of a fair analysis:

$$A_{circle} = \pi * R^2 = \pi * 56^2 \cong 9852 \text{ m}^2 \quad (5-3)$$

$$[9852 * 0.005] = [49.26] \cong 50 \text{ nodes} \quad (5-4)$$

Since the communication is usually made from outside of the field to the centre where the hub is, I will consider only the semicircle of the node range oriented to the hub. In this way, I assure that the nodes closer to the hub are in the routing table which results in node's memory savings.

To conclude, the routing table of each node will have 25 nodes' id with neighbours that have closer path length to the hub.

5.4 Energy Storage System

5.4.1 Supercapacitor

The supercapacitor choice for the simulations bases its model in [28]. The energy stored in a SC is presented in Equation (5-5) in Joules.

$$E_{sc} = \frac{1}{2} CV_{SC}^2 \text{ [J]} \quad (5-5)$$

C represents the rated capacitance of each SC in farads and V_{SC} is the voltage across the SC. In order to power a node, a 3.6 V voltage drop is required. Since the SC in [29] are rated at 2.3 V, two SCs are required in series to achieve the power supply of a node. Thus, Equation (5-5) changes to:

$$E_{stored} = \frac{1}{4} CV_{stored}^2 \text{ [J]} \quad (5-6)$$

The energy stored in two 4.7 F SCs in series is 15.3 J at 3.6 V. However, tolerances on the rated capacitance ($-20/+40\%$), as well as unusable voltages under 2 V reduce the maximum energy capacity usage of the SC nearly to 50%, so a 7.65 J SC has been considered for simulations purposes.

The SC leaked energy measured by the authors of [28] shows that the leakage is directly proportional to the residual energy. Therefore, and since the voltage variation of the SC voltage cannot be measured in simulation, an invariant leakage is assumed and represents the energy leakage per time slot:

$$SC_{leakage} = 0.0001 \text{ [J}/\tau] \quad (5-7)$$

where the notation $\text{[J}/\tau]$ means Joules per “time slot”.

This energy leakage is the mean leakage of the respective supercapacitor, and is based on [28].

It is assumed that the node cannot survive only powered by the SC. So the node is considered *dead* or *out-of-service* as soon as the battery reaches the end of its cycle lifetime.

5.4.2 Battery

It is used a low-capacity storage device to get faster results during the simulation. An RB with a maximum energy of 75 J as been considered and relies on a small battery size.

The RB cycle lifetime (L_C) starts with 1150 and decreases 0.5 after each discharge. This situation simulates a battery with a DoD of 50% based on [2].

5.5 Results

All the simulations run data packet dissemination with 24 bytes. This enables the transmission of enough information per packet for multi-sensoring environments. The energy consumption by the transceiver is based on [27] where the authors studied the Mica2dot sensor platform at 3 V, 4 MHz, 915 MHz transceiver with a transmitted power of 3 mW (5 dBm). The energy consumptions are presented in Table 5.3.

Table 5.3 - Characteristic Data for the Mica2dot Sensor Platform

Transceiver Mode	Energy Consumed per Byte
Energy to Transmit	59.2 $\mu\text{J}/\text{byte}$
Energy to Receive	28.6 $\mu\text{J}/\text{byte}$

5.5.1 Grid Deployment

5.5.1.1 Simulation A

Simulation A presents a simulation scenario where relay nodes are used, in other words, 50% of the network is generating data packets while the other 50% is for relay purposes only. The simulation assumptions are presented in Table 5.4.

Table 5.4 - Grid Deployment Setup for Simulation A

	SETUP
Time Slot	100 ms
Source Nodes	50%
Packet Generation	2 packets/s
Simulation Duration	20 minutes
Harvested Energy	0.1 mJ/ τ

The grid deployment simulation represents a careful and controlled scenario where nodes are placed separately. The data rate considered of two packets per seconds is only for simulation proposes and will test the sustainability of the network. A harvesting source of 0.1 mJ/ τ , which corresponds to 1 mW, is selected and corresponds nearly to an indoor photovoltaic cell condition. The source nodes represent the amount of nodes that generate a packet. In this simulation, 50% of the network is generating data packets where the others 50% only suits to route packets.

A combination of the SC residual energy with the RB residual energy is presented in Figure 5.3. The overall energy is gathered at the end of 20 minutes of network simulations.

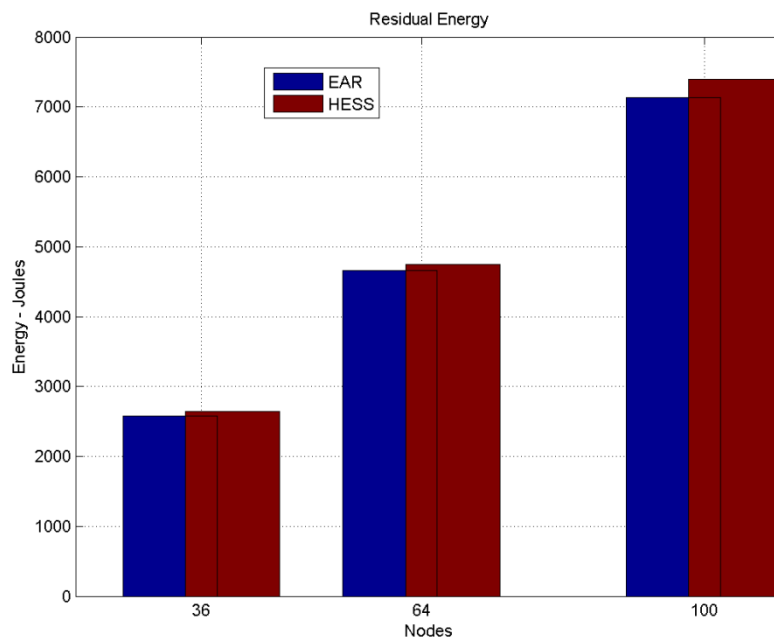


Figure 5.3 - Residual Energy for the Simulation A

The data packets successfully delivered to the hub are shown in Figure 5.4 and gathers the total amount of packets delivered in 20 m.

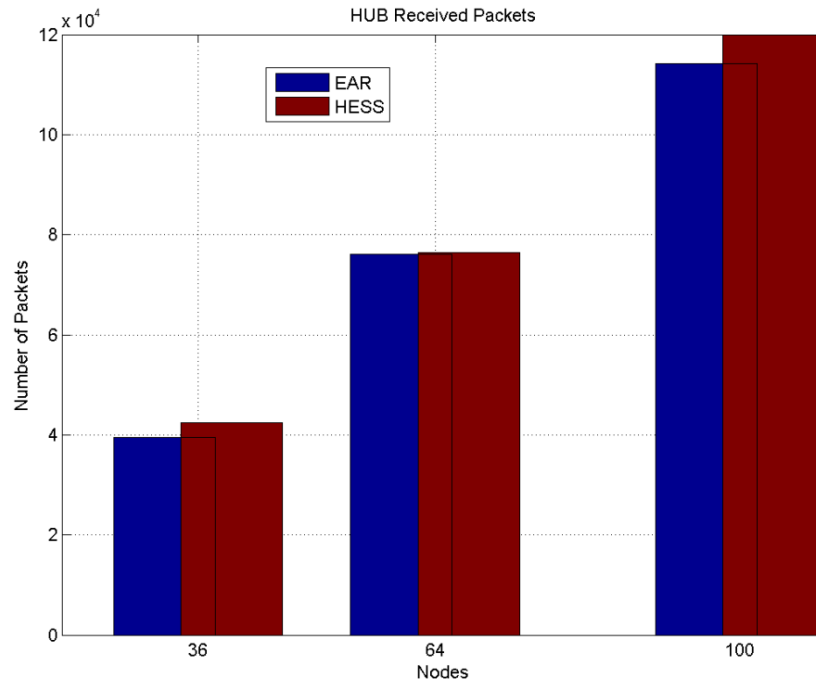


Figure 5.4 - Successful Packet for Simulation A

Even with a bigger amount of data packets delivered to the sink node, the total residual energy of the HESS protocol overcomes the EAR protocol. This corresponds to a better energy per data packet delivery.

Figure 5.5 and Figure 5.6 show the data packets delay in *hopcounts* and seconds. The results are averaged based on the total data packets received at the hub.

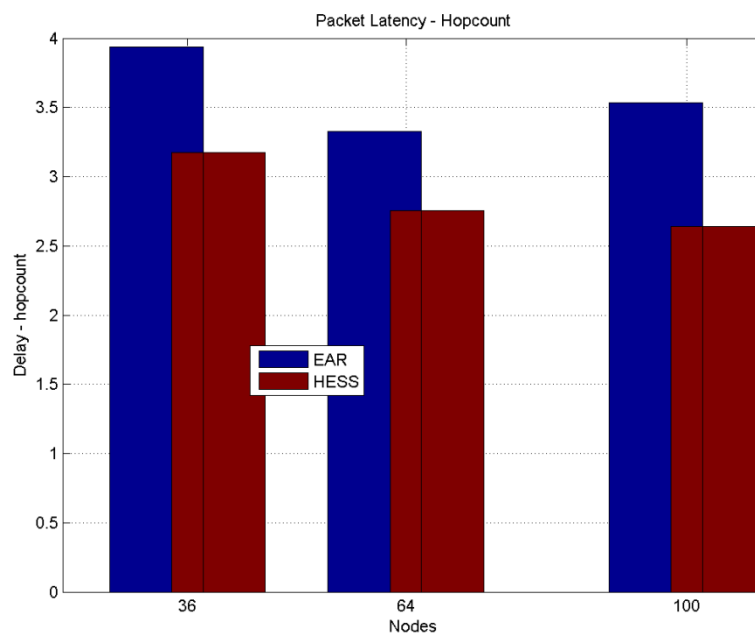


Figure 5.5 - Packet Delay in *Hopcounts* for Simulation A

In this simulation setup, the lowest network size presents a considerably larger packet latency which relies with the low node density of the network.

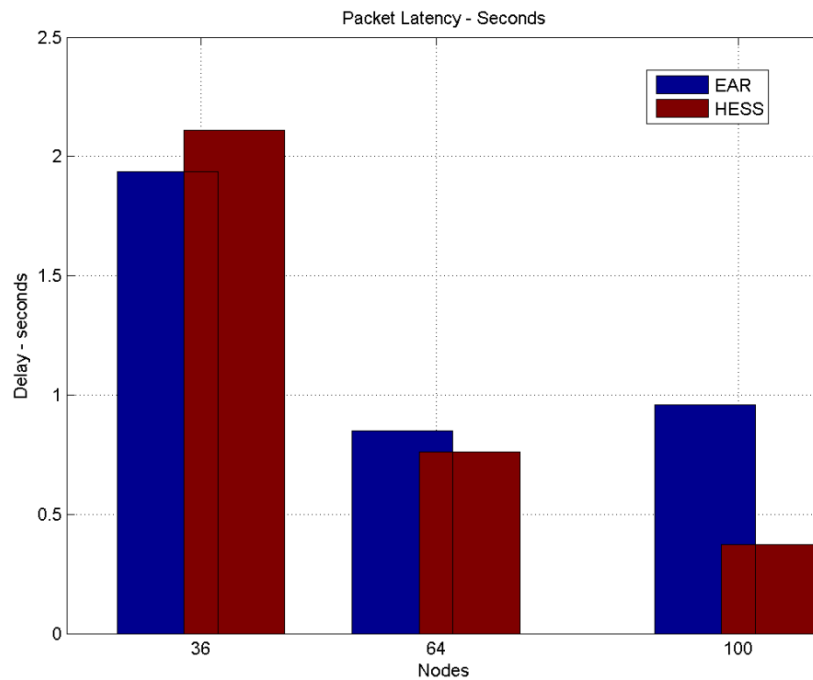


Figure 5.6 - Packet Delay in seconds for Simulation A

A selection of node monitoring has been made in order to verify the energy resources. Figure 5.7 shows the nodes that have been followed and monitored in a network size of 64 nodes.

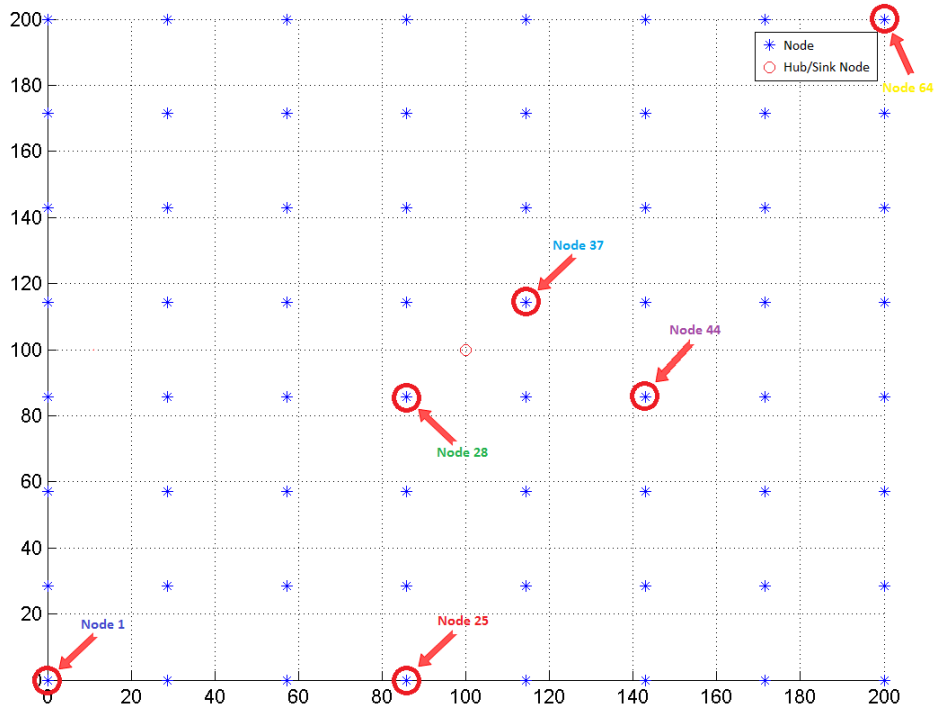


Figure 5.7 - Node Selection on a Grid Deployment

The monitoring of EAR SC residual energy during 12000 time slots is shown in Figure 5.8.

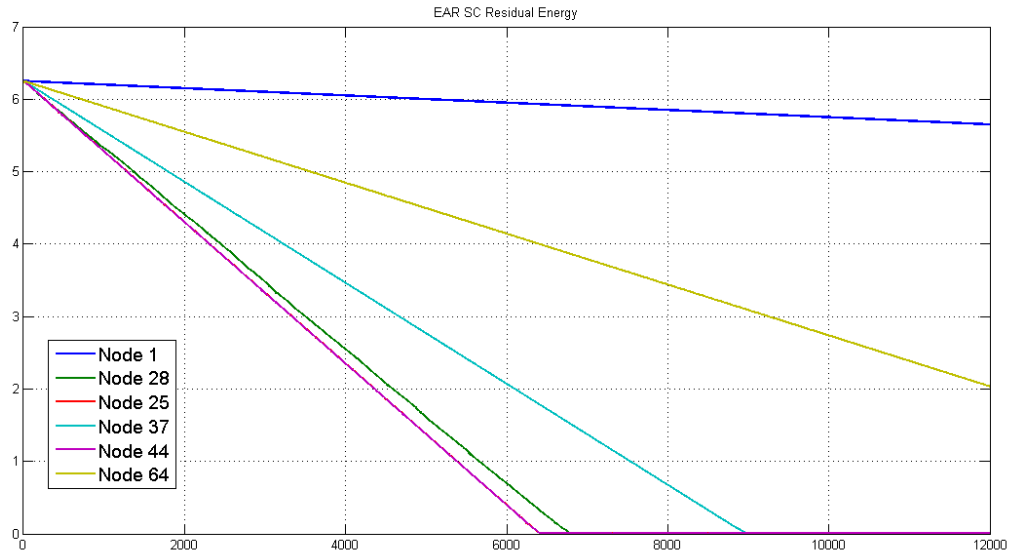


Figure 5.8 - EAR SC Residual Energy during 12000 Time Slots τ (20 min)

Both nodes 25 and 44 have coincident curves of SC residual energy in Figure 5.8.

The ability of HESS to sustain a longer network lifetime is presented in Figure 5.9 where the declivity of all nodes' residual energy is shown to be lower. However, the quick depletion of energy is considered a problem. The harvested energy cannot sustain the perpetual power nodes. This is due to the high data rate of source generation that cause high energy depletion on nodes that are closer to the sink node.

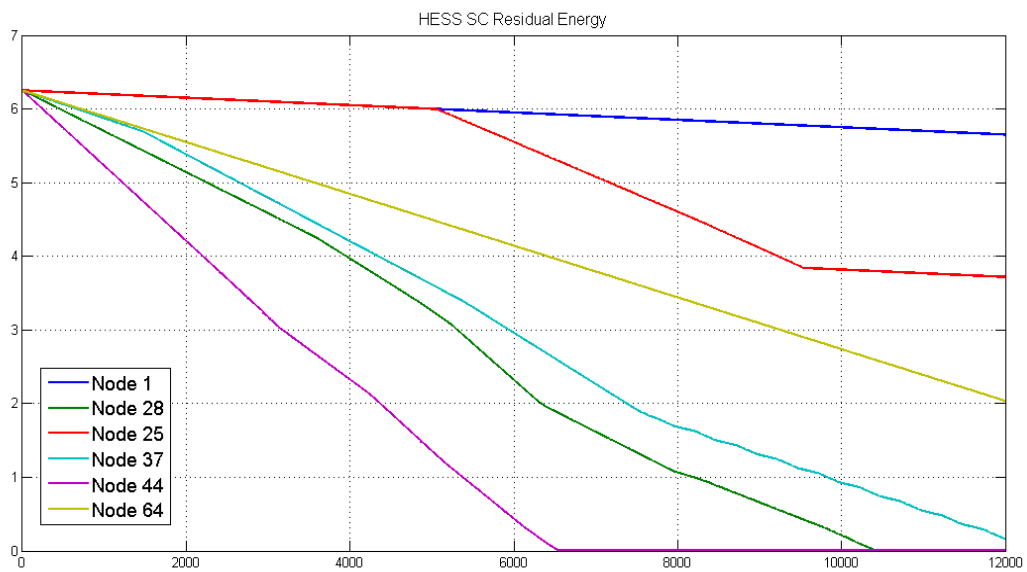


Figure 5.9 - HESS SC Residual Energy during 12000 Time Slots τ (20 min)

5.5.1.2 Simulation B

A similar study was made in simulation B by increasing the data packets generation to 100% of the network, in other words, every node of the network produces a packet each 500 ms and route it to the sink node. Table 5.5 presents the simulation assumptions for this scenario.

Table 5.5 - Grid Deployment Setup for Simulation B

	SETUP
Time Slot	100 ms
Source Nodes	100%
Packet Generation	2 packets/s
Simulation Duration	20 minutes
Harvested Energy	0.1 mJ/ τ

Simulation B uses a similar harvesting source which corresponds to an indoor photovoltaic cell.

The both EAR and HESS residual energies are shown in Figure 5.10.

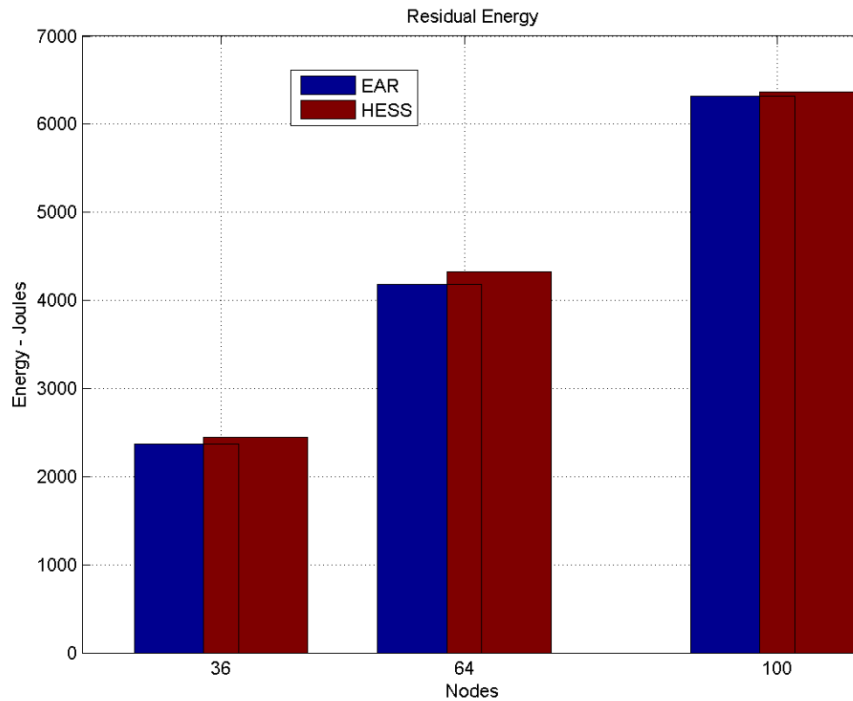


Figure 5.10 - Residual Energy for Simulation B

The HESS residual energy still overcomes the EAR protocol with similar success on delivering packets shown in Figure 5.11.

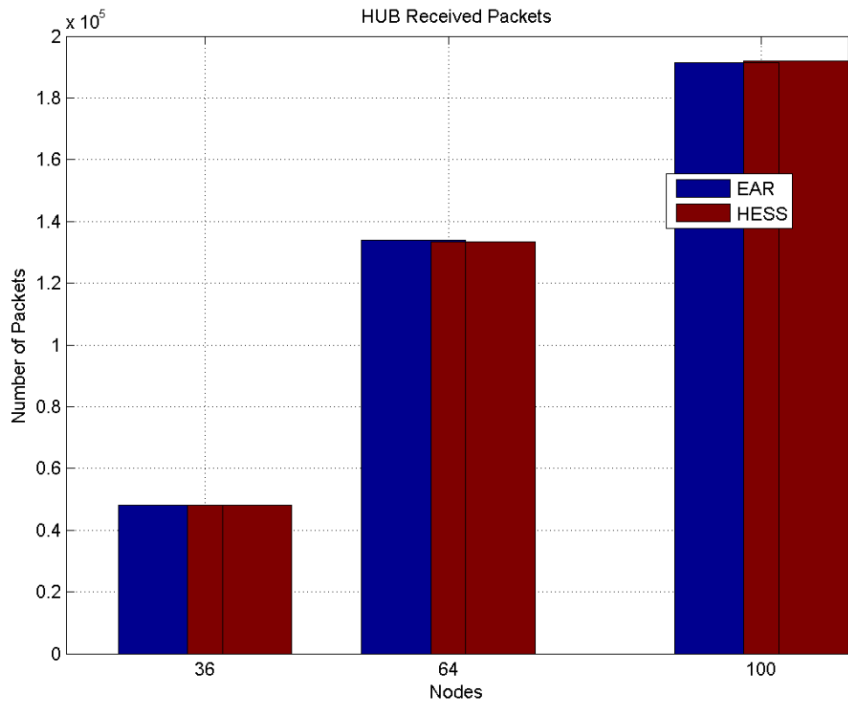


Figure 5.11 - Successful Packet Delivery for Simulation B

Figure 5.12 and Figure 5.13 show the packet latency in *hopcounts* and in seconds, respectively

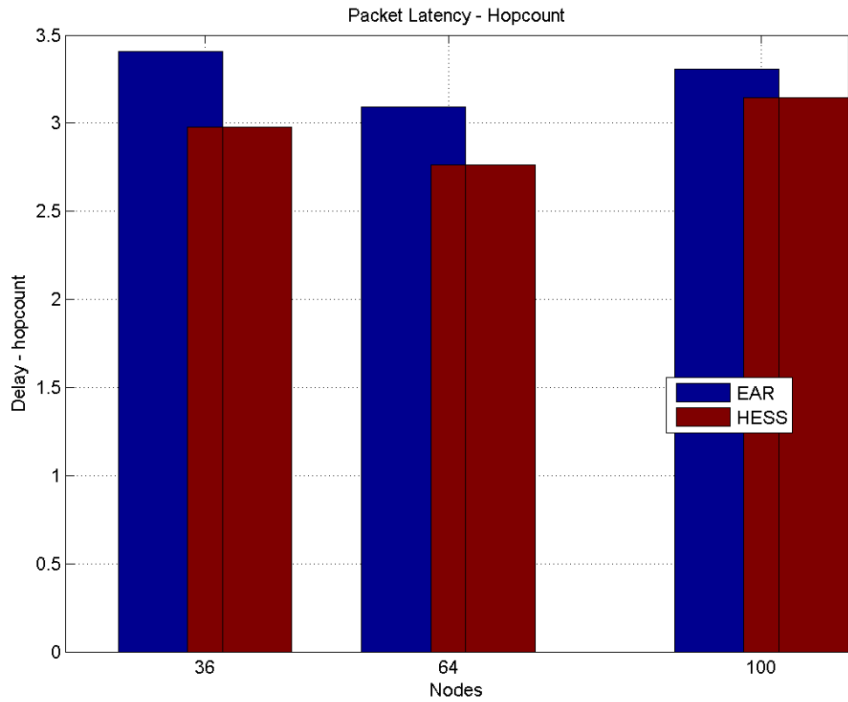


Figure 5.12 - Packet Delay in *Hopcounts* for Simulation B

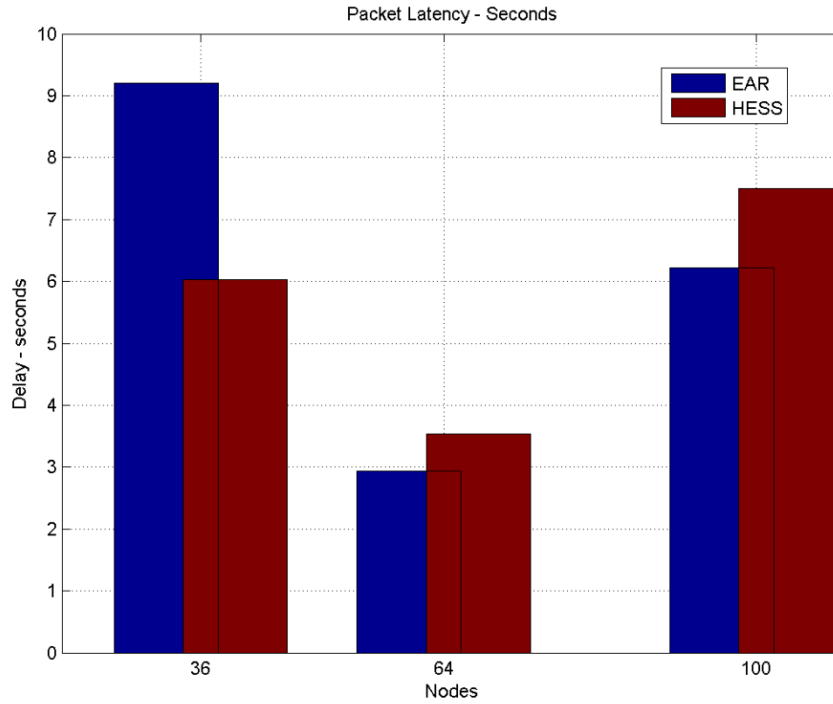


Figure 5.13 - Packet Delay in seconds for Simulation B

The packet latency remains the bigger problem with a small network size. However, the averaged delay of 7.5 s is reliable for such a large network size in a monitoring scenario. For real-time monitoring, a second sink node should be placed in the network deployment in order to get faster data packets delivery.

5.5.1.3 Simulation C

Simulation C presents another case of study where data packet rate is lower. Source nodes generate a packet each 10 s. An outdoor photovoltaic cell is used to harvest energy which produces 1 mJ per time slot. Table 5.6 presents the simulation assumptions for this scenario.

Table 5.6 - Grid Deployment Setup for Simulation C

	SETUP
Time Slot	100 ms
Source Nodes	100%
Packet Generation	6 packets/min
Simulation Duration	200 minutes
Harvested Energy	1 mJ/ τ

In this simulation, it is assumed that all the nodes harvest energy. With this data packet generation rate, the amount of energy harvested exceeds the amount of consumed energy, leading to a self-sustainable network. Figure 5.14 shows the total number of packets that the network routed.

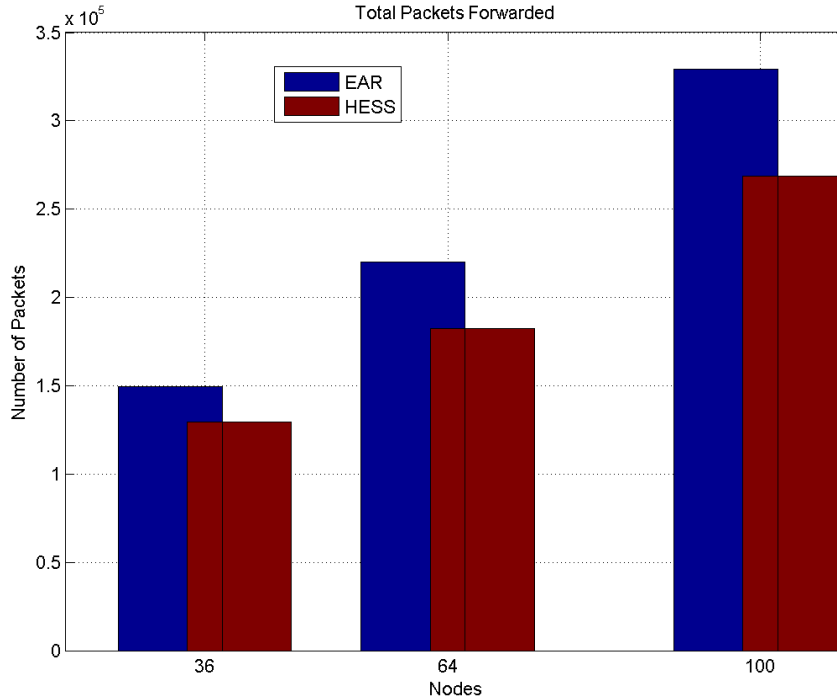


Figure 5.14 - Packets Forwarded for Simulation C

Both routing protocols, HESS and EAR, delivered the same amount of packets to the sink node. However, the HESS was able to deliver with less *hopcounts* and time latency as shown in Figure 5.15 and Figure 5.16.

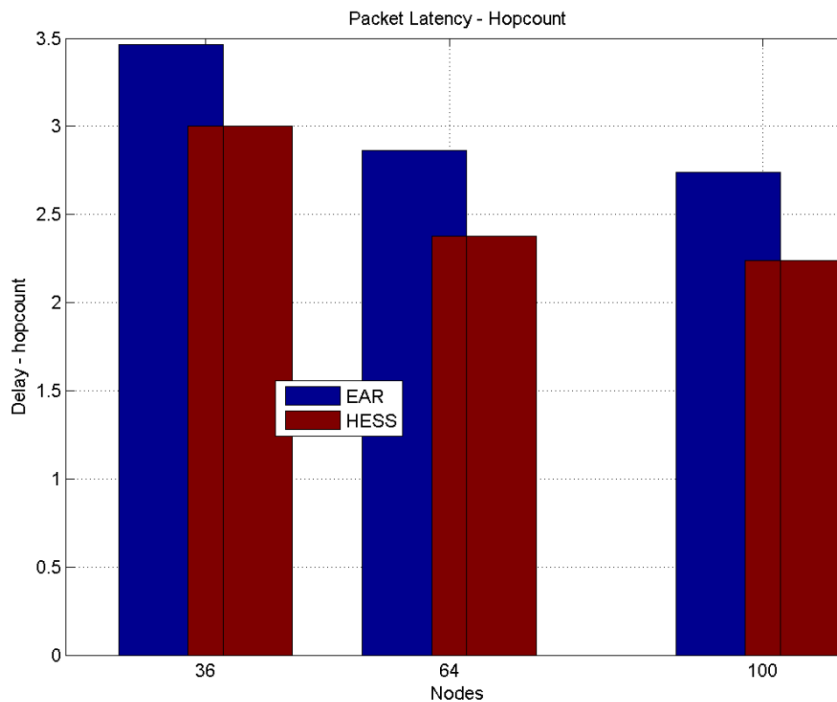


Figure 5.15 - Packet Delay in *Hopcounts* for Simulation C

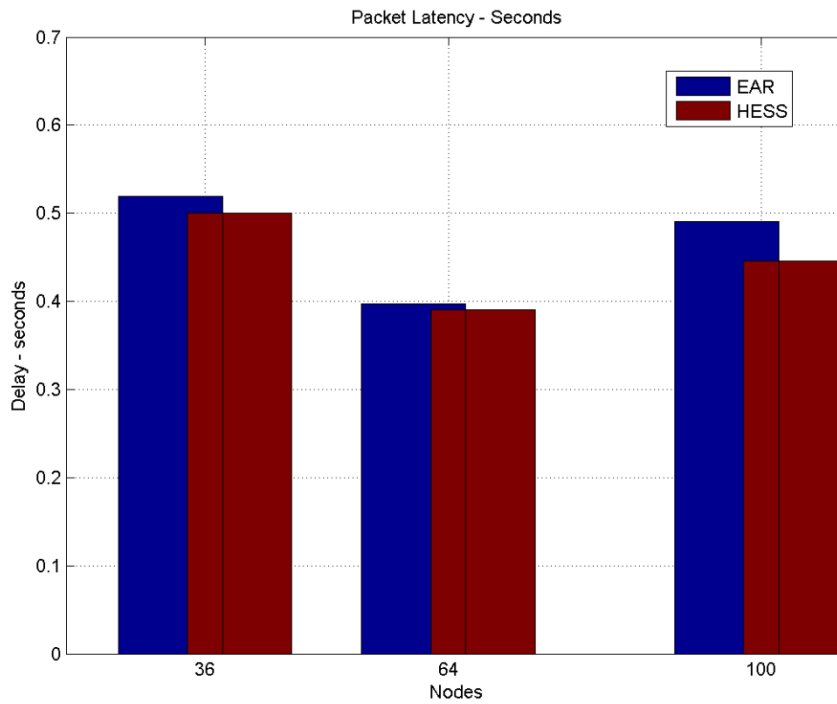


Figure 5.16 - Packet Delay in seconds for Simulation C

A higher delay was observed for small size networks (36 nodes) because of the smaller node density which leads to fewer neighbours in the routing table. With fewer neighbours, data packets are routed through the same path resulting in bigger data queue and more delay.

5.5.1.4 Simulation D

This simulation presents a scenario with source nodes generating a packet per second. A higher data packet generation rate is analysed with only 50% of nodes harvesting at each time slot. Table 5.7 presents the simulation setup for this scenario.

Table 5.7 - Grid Deployment Setup for Simulation D

	SETUP
Time Slot	100 ms
Source Nodes	100%
Packet Generation	1 packet/second
Simulation Duration	60 minutes
Harvested Energy	1 mJ/ τ

Figure 5.17 and Figure 5.18 show the packet delay in *hopcounts* and time delay in seconds, respectively.

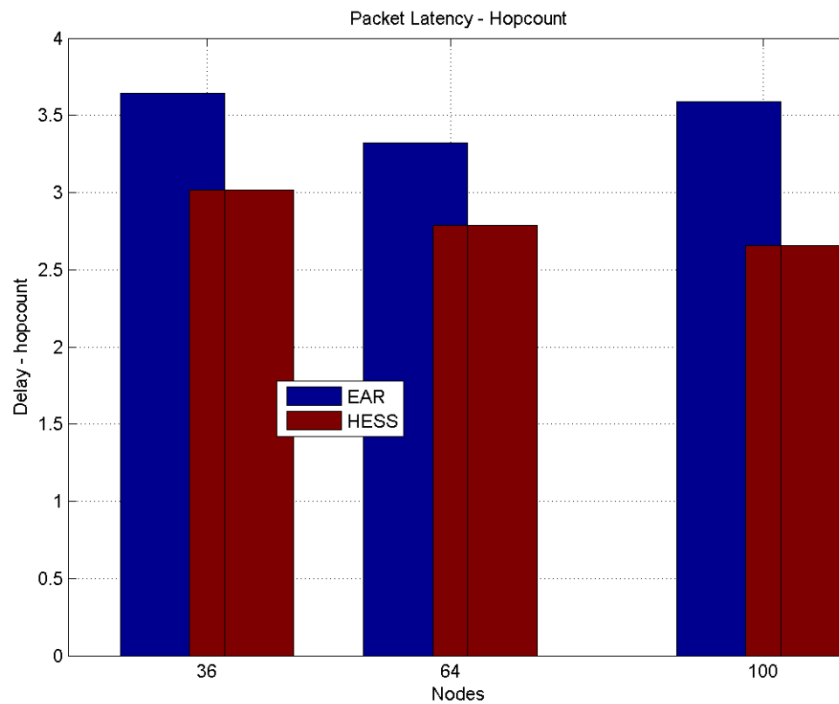


Figure 5.17 - Packet Delay in *Hopcounts* for Simulation D

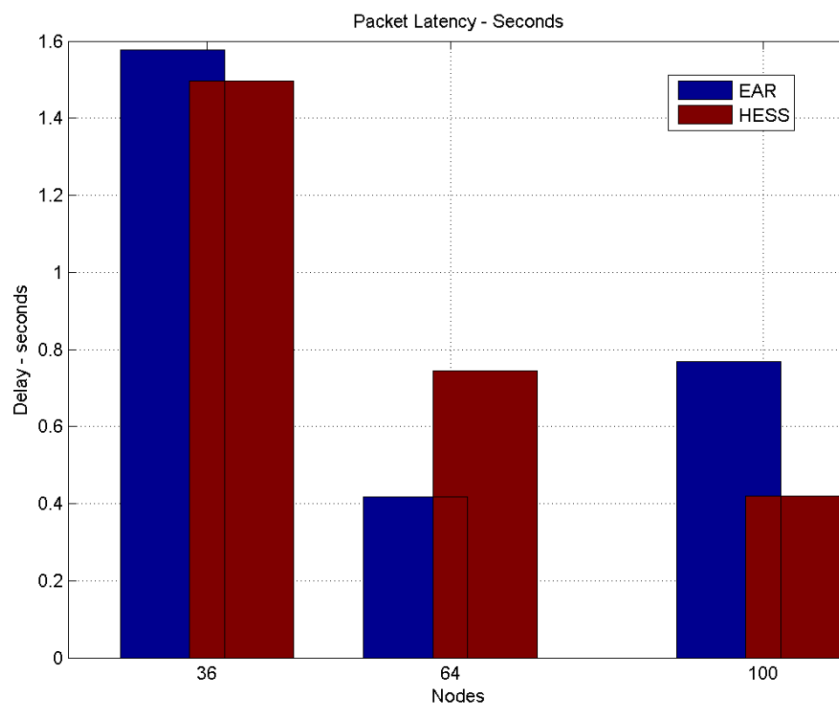


Figure 5.18- Packet Delay in seconds for Simulation D

The packet delay shows a slower data delivery when crowded networks generate huge amount of packet. This leads to quick network

exhaustion in EAR protocol. However, a balanced and distributed data routing is carried on by HESS protocol.

In a 50% harvesting scenario, the transmission load of HESS is balanced which enables careful consumption ability. Figure 5.19 presents the residual energy distribution at the end of 60 minutes simulation. The residual energy is obtained by the following equation:

$$HESS_{energy} = \sum_{n=64}^{n=1} \frac{(e_{SC}(n) + e_{RB}(n)) * 100}{81.25} \quad (5-8)$$

$$EAR_{energy} = \sum_{n=64}^{n=1} \frac{(e_{SC}(n) + e_{RB}(n)) * 100}{81.25} \quad (5-9)$$

Where the energy at the beginning of the simulation is:

$$81.25 J = u_{SC} + u_{RB}. \quad (5-10)$$

Then, the residual energy differential in percentage is given by:

$$HESS_{energy} - EAR_{energy} \quad (5-11)$$

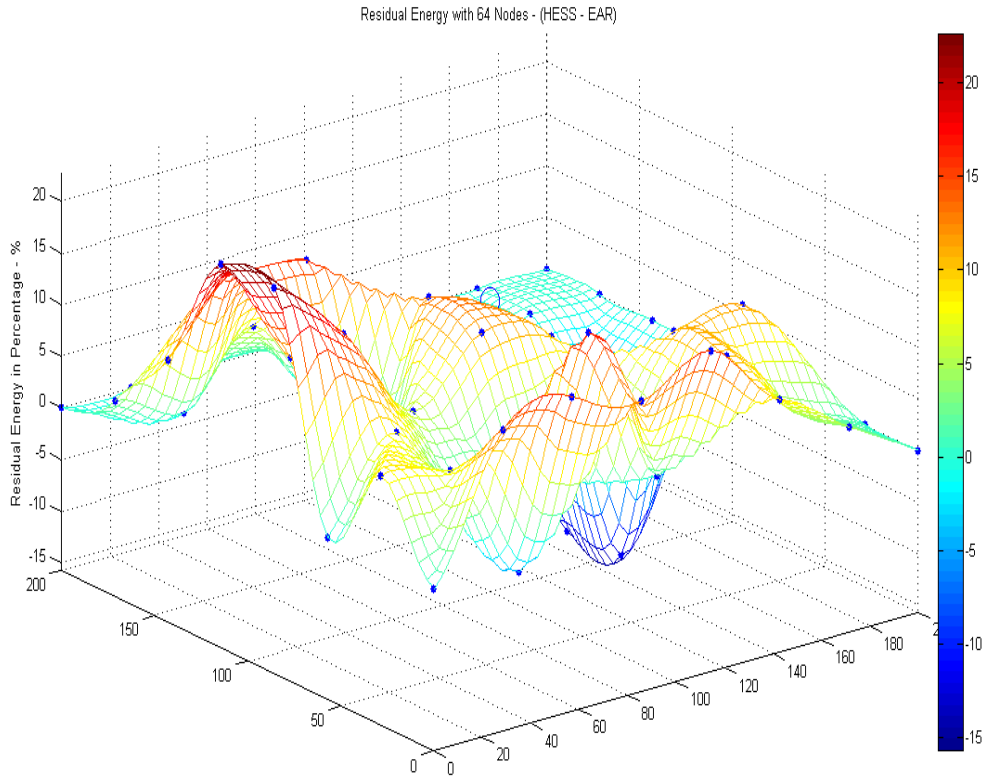


Figure 5.19 - Differential Residual Energy with 64 Nodes

5.5.2 Random Deployment

The random node deployment, as explained in Section 5.2 represents an airplane distribution. The simulation assumptions are show in Table 5.8.

Table 5.8 - Random Deployment Setup

	SETUP
Iterations	5
Time Slot	100 ms
Source Nodes	50%
Packet Generation	2 packets/s
Simulation Duration	60 minutes
Harvested Energy	0.1 mJ/ τ

The source nodes generate data packets that are routed to the sink node. In this 60 minutes simulation, the total packet generated per source node is 7200 with a rate of 2 packets per second.

The harvested energy relies on an energy source that produces 1 mW which is based on an outdoor photovoltaic cell.

The results represent five averaged runs with the same network size but different node distribution. The total residual energy is presented in Figure 5.20.

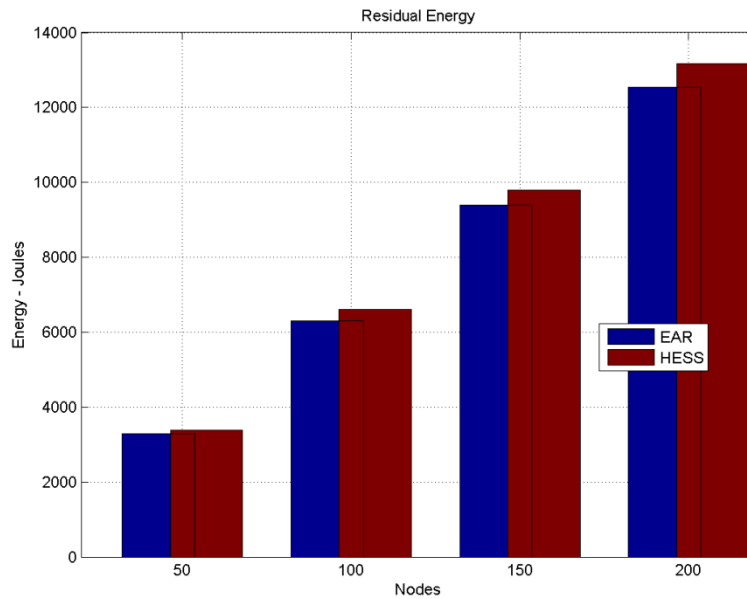


Figure 5.20 - Random Deployment Residual Energy

The residual energy gathers all nodes residual energy at the end of the simulation time ($e_{rb} + e_{sc}$). The results show that the HESS protocol can

perform better energy consumption since it has more energy with almost the same amount of packet deliveries.

Figure 5.21 shows the hub received packets which are, as previously explained, packets that were successfully delivered to the hub/sink node.

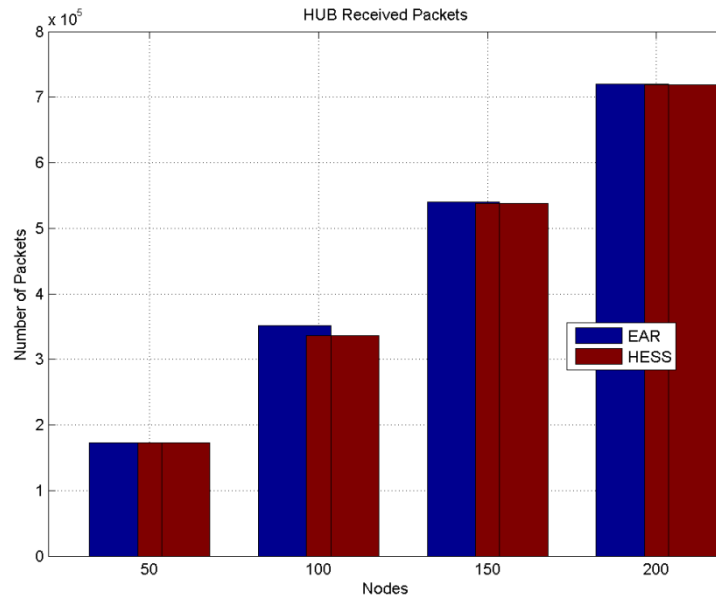


Figure 5.21 - Random Deployment Successful Packet

Figure 5.22 represents the packet delay. The delay is presented in *hopcounts* or, in other words, the number of hops that a packet is routed until it reaches the hub/sink node. The results are averaged over the five runs.

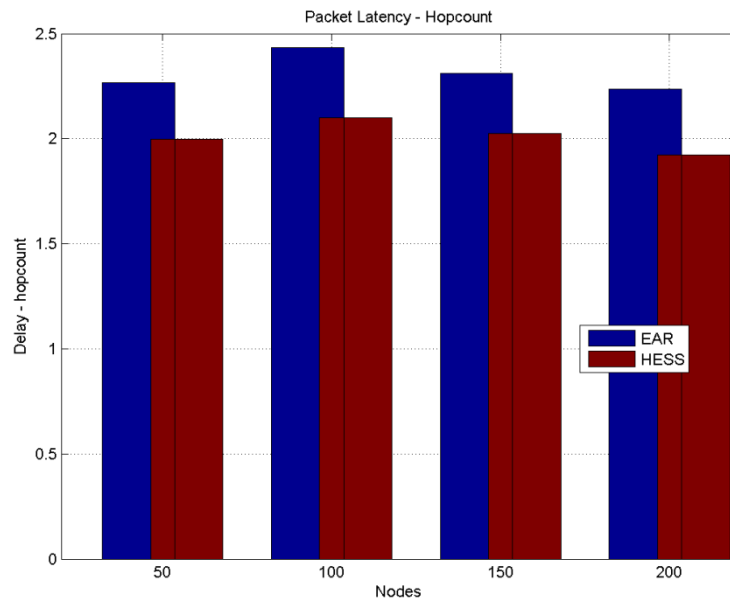


Figure 5.22 - Random Deployment Packet Delay in Hopcounts

A better packet latency of about 0.5 hops is presented in the previous figure. The second delay measurement uses the time delay between the data generation and the delivery to the sink node and is presented in Figure 5.23.

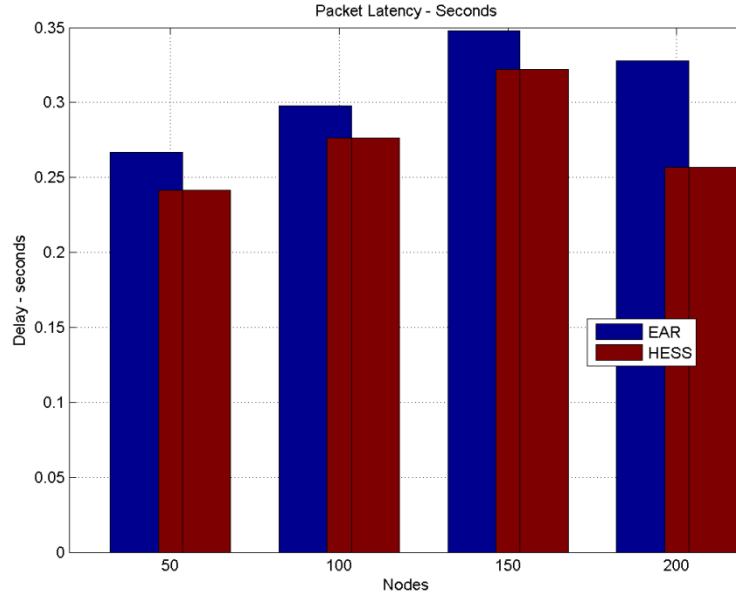


Figure 5.23 - Random Deployment Packet Delay in Seconds

The previous plot shows the average delay at which the packets arrived at the hub in seconds. It is important to remember that each time slot corresponds to 100 ms. An important performance is shown with crowded network size (200 nodes) were HESS protocol packets reach the sink node with less 0.8 s than EAR packets.

5.6 Summary

The simulations presented in this Chapter show different setups were the routing protocols are analysed. Several analyses assure a better result by using the HESS protocol when compared with EAR. The use of a hybrid energy storage system enables the network lifetime extension. However, an important energy leakage occurs when a SC is used in the energy system. The amount of energy wasted in current leakage by the SC requires a harvesting source and a node design that overcomes the node energy demand. Simulations A and B reproduce this scenario by having an intense data packet generation with a low energy source. This leads to a quickly exhaustion of the backbone nodes and then, to the end of the network lifetime. A multi-sink node scenario can be used for such crowded network by creating different transmission flows and balancing the energy consumption of the network.

A self-sustainable network is only reached when the harvesting energy overcomes the node consumption. This occurs in simulations C and D where a low data generation scenario is applied to a powerful energy source.

6. Conclusions and Future Works

This work provides an overview of the present work done in hybrid energy storage systems applied to WSNs.

The Chapter 2 presents the related work on the different part of the topic of research. The lake of works on hybrid energy storage systems provided a good opportunity for the selection of this research topic. The main energy sources that can actually be applied to WSNs are shown in Table 2.2. It is represented a set of harvesting sources available in the diverse application scenarios. The limited energy provided by the harvesting devices is one of the main restrictions that contains the use of harvesting devices in WSN. Different scenarios demand different energy requirements where the transceiver has always the largest energy consumption. This narrows the selection of possible energy sources that fulfil the network self-sustainability. Therefore, one way to optimize the energy consumption caused by data transmission is choosing an energy-aware routing protocol that efficiently route data packets through the network. The Chapter 3 describes a simple and Energy-Aware Routing (EAR) protocol that routes data packets considering the residual energy in each node. It is shown that this approach does not consider the harvesting process on which, this thesis relies. Therefore, HESS cost function metrics are presented in Chapter 4, covering the several residual energy levels as well as other determinant factors to achieve an enhanced routing in a hybrid energy storage system with energy harvesting. The power management unit is also reviewed in this Chapter 4 and results in a new switching interface that optimizes the energy flow between energy storages and the load. The HESS metric flexibility proves to perform the extension of the network lifetime in different application scenarios analysed in Chapter 5. This Chapter also provides a comparative analysis between EAR and HESS protocols considering the packet delay taking into account the *hopcounts* and the time spent in successful packet deliveries.

Some more works could have been done in this project. But due to the limitation in time, the adaptation process to a new working environment as well as prolonged MATLAB simulations, some results could not be presented in this report.

A detailed analysis could be carried on in order to tune the cost function weights. This would take advantage of the HESS protocol flexibility and fit the network demand in different scenarios. Genetic algorithm analysis would be one of the suitable methods to perform the weights adaptation to different application requirements. A long run simulation could also be performed in order to simulate the RB cycle life behaviour when using different depth of discharge (DoD) settings.

Furthermore, this project could also be extended to a real life implementation where nodes with SC and RB energy storage would be

monitored. This analysis would allow the comparison between the simulation results and the practical ones.

7. Bibliography

- [1] X. Jiang, J. Polastre, and D. Culler, "Perpetual Environmentally Powered Sensor Networks," in *4th Int'l Conf. Information Processing in Sensor Networks*, Los Angeles, CA, 2005.
- [2] (2005) Battery Performance Characteristics. [Online]. <http://www.mpoweruk.com/life.htm#dod>
- [3] W. R. Heinzelman, A. Chandrakasan, and H. Balakrishnan, "Energy Efficient Communication Protocol for Wireless Microsensor Networks," in *Proceedings of the 33rd IEEE Hawaii International Conference on System Sciences (HICSS)*, Jan. 2000, pp. 1-10.
- [4] S. Basagni, C. Petrioli, and R. Petrocchia, "Efficiently Reconfigurable Backbones for Wireless Sensor Networks," *Computer Communications*, vol. 31, pp. 668-698, March 2008.
- [5] J. N. Al-Karaki and A. E. Kamal, "Routing Techniques in Wireless Sensor Networks: A Survey," *IEEE Wireless Communications*, vol. 11, No. 6, pp. 6-28, 2004.
- [6] S. C. Ergen, "ZigBee/IEEE802.15.4 Summary," 2004.
- [7] H. Abusaimh and S.-H. Yang, "Balancing the Power Consumption Speed in Flat and Hierarchical WSN," *International Journal of Automation and Computing*, vol. 5, No. 4, pp. 366-375, October 2008.
- [8] (2001) Choosing a Rechargeable Battery. http://electusdistribution.com.au/images_uploaded/recharge.pdf.
- [9] I. Buchmann. Discharge Methods. [Online]. <http://www.batteryuniversity.com/partone-16.htm>
- [10] R. N. Torah, P. Glynne-Jones, M. J. Tudor, and S. P. Beeby, "Energy Aware Wireless Microsystems Powered by Vibration Energy Harvesting," in *PowerMEMS*, Freiburg, Germany, 2007.
- [11] (2006) Battery University, Practical Battery knowledge for Engineers, Educators, Students and Battery Users Alike. [Online]. <http://www.batteryuniversity.com>
- [12] J. M. Gilbert and F. Balouchi, "Comparison of Energy Harvesting Systems for Wireless Sensor Networks," *International Journal of Automation and Computing*, vol. 5, N. 4, pp. 334-347, October 2008.
- [13] L. Lin, N. B. Shroff, and R. Srikant, "Asymptotically Optimal Power-Aware Routing for Multihop Wireless Networks with Renewable Energy Sources," *IEEE/ACM Transactions on Networking*, vol. 2, Issue 5, pp. 1021-1034, October 2007.
- [14] L. Palma, P. Enjeti, and J.W. Howze, "An Approach to Improve Battery Run-time in Mobile Applications with Supercapacitors," in *Power*

- Electronics Specialist Conference, PESC '03*, vol. 2, pp. 912-923, June 2003.
- [15] R. A. Dougal, S. Liu, and R. E. White, "Power and Life Extension of Battery-Ultracapacitor Hybrids," *IEEE Transactions on Components and Packaging Technologies*, vol. 25, No. 1, pp. 120-131, March 2002.
 - [16] M. A. Ingram, Y. Zang, and A. Kailas, "Communications using Hybrid Energy Storage Systems, and Cooperative Harvesting and Transmission," Georgia Institute of Technology, DRAFT v.3.
 - [17] S. Hedetniemi and A. Liestman, "A Survey of Gossiping and Broadcasting in Communication Networks," *IEEE Networks*, pp. 319-349, 1988.
 - [18] A. Scaglione and Y. W. Hong, "Opportunistic large arrays: cooperative transmission in wireless multihop ad hoc networks to reach far distances," *IEEE Transactions on Signal Processing*, pp. 2082-2092, August 2003.
 - [19] L. V. Thanayankizil, A. Kailas, and M. A. Ingram, "Two Energy-Saving Schemes for Cooperative Transmission with Opportunistic Large Arrays," in *IEEE GLOBECOM*, 2007, pp. 1038-1042.
 - [20] K. Akkaya and M. Younis, "A Survey on Routing Protocols for Wireless Sensor Networks," *Ad Hoc Networks*, vol. 3, No. 3, pp. 325-349, May 2005.
 - [21] J. Kulik, W. Heinzelman, and H. Balakrishnan, "Negotiation-Based Protocols for Disseminating Information in Wireless Sensor Networks," in *Mobicom'99*, vol. 8, 2002, pp. 169-185.
 - [22] C. Intanagonwiwat, R. Govindan, D. Estrin, J. Heidemann, and F. Silva, "Directed Diffusion for Wireless Sensor Networking," *IEEE/ACM Transactions on Networking*, vol. Volume 11, Issue 1, pp. 2-16, February 2003.
 - [23] C. E. Perkins and E. M. Royer, "Ad hoc On-Demand Distance Vector Routing," in *Proceedings of the 2nd IEEE Workshop on Mobile Computing Systems and Applications*, 1999, pp. 90-100.
 - [24] Huan L. and Yi P. Keong L., "An Efficient and Reliable Routing Protocol for Wireless Sensor Networks," *Proceedings of the First International IEEE WoWMoM Workshop on Autonomic Communications and Computing (ACC'05)*, vol. 02, 2005.
 - [25] A. Kailas and M. A. Ingram, "A Novel Routing Metric for Environmentally-Powered Sensors With Hybrid Energy Storage Systems," *Wireless VITAE Conference*, 2009.
 - [26] I. F. Akyildiz, W. Su, Y. Sankarasubramaniam, and E. Cayirci, "Wireless Sensor Networks: A Survey," *Computer Networks*, vol. 2, pp. 393-422, 2002.

- [27] P. Trakadas, T. Zahariadis, H. C. Leligou, S. Voliotis, and K. Papadopoulos, "Analyzing Energy and Time Overhead of Security Mechanisms in Wireless Sensor Networks," in *15th International Conference on Systems, Signals and Image Processing*, 2008, pp. 1137-140.
- [28] G. V. Merrett et al., "An Empirical Energy Model for Supercapacitor Powered Wireless Sensor Nodes," in *17th International IEEE Conference on Computer Communications and Networks*, Virgin Islands (USA), 2008.
- [29] Panasonic, *Gold Capacitors Technical Guide.*, 2005.

8. Appendix

8.1 Appendix A: MATLAB Code Description

The MATLAB code, attached to the Master thesis report in digital format, is divided into two major parts. The first relies on the nodes' deployment and the routing setup phase that, as explained in Chapter 3, is responsible for the neighbouring detection and routing tables' replenishment. The second part of the MATLAB code includes both routing protocol framework (EAR and HESS) which after setting the assumption criteria, route data packets through the network.

8.1.1 Node Deployment Setup

The node deployment setup code is the starting point of all routing process. It is composed by *main.m* script which gathers all functions used in this stage. Right after setting the setups (network size, area length, etc), it calls function *deploy_node.m* which distributes the nodes within an area and returns a matrix with each node's placement. The next step is the ADV broadcast that, as explained in detail in Section 3.2.1, fulfil the routing tables of the first ring nodes, neighbours within the coverage area of the sink node. This step is accomplished by the function *adv_broadcast.m* which sets the first routing tables. The function *setup_phase.m* manages the hub broadcast as well as the function *rreq_broadcast.m* which performs the routing table replenishment of the rest of the network. The function *dist_calc.m* assures the data link coverage by using the Pythagoras Theorem.

The node deployment setup code returns raw data with matrixes that have information about the nodes' placement and initial energy.

8.1.2 Routing Protocols Framework

Both EAR and HESS protocol share a common name in the MATLAB code. Both have an initial script (*EAR_script.m* and *HESS_script.m*) that uses the preliminary setups in order to route data (source node percentage, simulation duration, etc). Therefore, the routing functions (*EAR_routing.m* and *HESS_routing.m*) are called by the script which actually performs the data routing of the network. These last functions have also some setup settings that relies on the harvesting rate, harvesting energy, etc. The function *c_energy.m* is called whenever an energy update must be performed.

The HESS protocol has an additional function named *cost_f.m* which calculates the cost of routing a packet through a node each time a communication is required.

The routing functions save essential variables in raw files to further analysis.